Geologica Acta, Vol.14, Nº 2, June 2016, 79-100
DOI: 10.1344/GeologicaActa2016.14.2.1

Gas hydrates distribution in the Shenhu area, northern South China Sea: comparisons between the eight drilling sites with gas-hydrate petroleum system

M. SU[1,2,3] R. YANG[1,2,3] H. WANG[4] Z. SHA[4,5*] J. LIANG[4] N. WU[6] S. QIAO[1,2,3] X. CONG[1,2,3]

[1]Key Laboratory of Gas Hydrate, Chinese Academy of Sciences
Guangzhou Guangdong, 510640, China

[2]Guangzhou Key Laboratory of New and Renewable Energy Research and Development
Guangzhou Guangdong, 510640, China

[3] Guangzhou Institute of Energy Conversion, Chinese Academy of Sciences
Guangzhou Guangdong, 510301, China

[4]Guangzhou Marine Geological Survey
Guangzhou Guangdong, 510075, China

[5]Faculty of Earth Resources, China University of Geosciences
Wuhan Hubei, 430074, China

[6]Key Laboratory of Gas Hydrate, Ministry of Land and Resources
Qindao Shandong, 266071, China

*Corresponding author

ABSTRACT

The results of the first marine gas hydrate drilling expedition of Guangzhou Marine Geological Survey (GMGS-1) in northern continental slope of the South China Sea revealed a variable distribution of gas hydrates in the Shenhu area. In this study, comparisons between the eight sites with gas-hydrate petroleum system were used to analyze and re-examine hydrate potential. In the Shenhu gas hydrate drilling area, all the sites were located in a suitable low-temperature, high-pressure environment. Biogenic and thermogenic gases contributed to the formation of hydrates. Gas chimneys and some small-scale faults (or micro-scale fractures) compose the migration pathways for gas-bearing fluids. Between these sites, there are three key differences: the seafloor temperatures and pressures; geothermal gradient and sedimentary conditions. Variations of seafloor temperatures and pressures related to water depths and geothermal gradient would lead to changes in the thickness of gas hydrate stability zones. Although the lithology and grain size of the sediments were similar, two distinct sedimentary units were identified for the first time through seismic interpretation, analysis of deep-water sedimentary processes, and the Cm pattern (plotted one-percentile and median values from grain-size analyses), implying the heterogeneous sedimentary conditions above Bottom Simulating Reflectors (BSRs). Based on the analyses of forming mechanisms and sedimentary processes, these two fine-grained sedimentary units have different physical properties. Fine-grained turbidites (Unit I) with thin-bedded chaotic reflectors at the bottom acted as the host rocks for hydrates; whereas, fine-grained sediments related to soft-sediment deformation (Unit II) characterized by thick continuous reflectors at the top would serve as regional homogeneous caprocks. Low-flux methane that migrated upwards along chimneys could be enriched preferentially in fine-grained turbidites, resulting in the formation of hydrates within Unit I.

However, overlying fine-grained sediments related to soft-sediment deformation would hinder the further migration of gases/fluids, causing the extremely low methane concentration in Unit I. Three of the eight sites with hydrates from recovered core samples were located within sedimentary Unit I, and the other five sites were not. Because, the most significant difference between the eight sites is the nature and type of sedimentary deposits above the BSRs, it is suggested therefore that sedimentary conditions are the crucial factor controlling the formation and occurrence of gas hydrates in the Shenhu gas hydrate drilling area, northern South China Sea.

KEYWORDS | **Gas hydrate. Variable distribution. Gas-hydrate petroleum system. Shenhu area. Northern South China Sea.**

INTRODUCTION

Gas hydrates are naturally occurring ice-like crystalline substances that consist of water and natural gases (*e.g.*, methane, ethane, and carbon dioxide) stable under low-temperature and high-pressure conditions (Kvenvolden, 1993; Sloan and Koh, 2008). They are widespread in permafrost regions and in sedimentary layers of the semi-deep to deep water environment (>300m depth) (Kvenvolden, 1998; Collett, 2002). Gas hydrates have recently been the subject of considerable attention due to their potential impacts on the global economy, society, and environment, particularly in relation to energy alternatives, global climate changes, and submarine geohazards (Dickens *et al.*, 1995; Dickens, 2003; Hesse, 2003; Klauda and Sandler, 2005; Maslin *et al.*, 2004; Milkov, 2004; Sultan *et al.*, 2004; Wallmann *et al.*, 2012).

Recently, some exploration activities involving marine gas hydrates have indicated that the distributions of gas hydrates are markedly variable. For examples, hydrates recovered in Nankai Trough were primarily trapped in turbidites known as the hydrate accumulation zones (Colwell *et al.*, 2004; Noguchi *et al.*, 2011; Tsuji *et al.*, 2004); the drilling sites located at Walker Ridge 313, Green canyon 955, and Alaminos canyon 21 during the Gulf of Mexico Gas Hydrate Joint Industry Project Leg II illustrated that the occurrences of hydrates were controlled by salt diapirs, faults, and sand-rich turbidites (Lee and Collett, 2012; Boswell *et al.*, 2012a, 2012b; Miller *et al.*, 2012); and drilling results in Ulleung Basin documented that hydrates accumulated within Mass Transport Complex (MTC) and fractures in gas chimneys (Chun *et al.*, 2011; Riedel *et al.*, 2012; Scholz *et al.*, 2012). The investigations of gas hydrates in India (the India National Gas Hydrate Program, INGHP) also showed spatially variable distributions, as no hydrates were recovered from the sites NGHP-01-02 and NGHP-01-03 with obvious Bottom Simulating Reflectors (BSRs) (Sain and Gupta, 2012). On the basis of summarization the occurrences of global gas hydrates, the concept of gas-hydrate petroleum system was proposed and used to understand the formation of hydrates in both permafrost regions and marine environments (Collett, 2009). Highlighting physical/chemical conditions (temperature, pressure, gas composition, and availability of water) and geological settings (gas-bearing fluid migration and sedimentary condition), gas-hydrate petroleum system could be seen as a systematical method to assess the gas hydrate potential and outline the controlling factors of its occurrence (Rajan *et al.*, 2013; Riedel *et al.*, 2013a).

In this study, we use a case study to illustrate the variability in distribution of gas hydrates in the Shenhu area, northern continental slope of the South China Sea (Fig. 1), where the first marine gas hydrate drilling expedition (GMGS-1) organized by Guangzhou Marine Geological Survey (GMGS) was conducted from 18 April to 11 June 2007. Hydrate-bearing samples during GMGS-1 were recovered at only SH2, SH3 and SH7 of the eight drilling sites (Fig. 2) (Wu *et al.*, 2008; Yang *et al.*, 2008). Log data showed that such gas-hydrates were present in thin-bedded sand-rich sedimentary packages (Wang *et al.*, 2014a). Previously, a number of geological models have been proposed to explain this variability of gas hydrate distribution in the Shenhu area. One model used, heat flow values, measured by a Dorado-I Multichannel Heat Flux Probe and a Fugro Pore Water Sampler System, to describe the formation of a late-stage mud diapir to develop at site SH5, causing the complete dissociation of hydrates and leading to the absence of hydrates at this site (Li *et al.*, 2010; Wang *et al.*, 2010; Xu *et al.*, 2012). Chen *et al.* (2011) developed a relationship between the saturation of gas hydrates and sedimentary grain size at sites SH2 and SH7. Furthermore, the presence of abundant foraminifera could increase the porosity of fine-grained sediments, thus exerting a strong influence on the accumulation of hydrates (Chen *et al.*, 2013b). Sun *et al.* (2012a, b), (Chen *et al.*, 2013a) and Yang *et al.* (2015) proposed that gas chimneys from seismic data at site SH2 could provide a migration pathway for gases/fluids and create a network fractures allowing the formation of hydrates in fine-grained sediments. Wang *et al.* (2014b) integrated seismic data, well logs, and cores of all the eight sites, concluding that thermogenic source and upward migration of gases/fluids from the deeper sediment layers were reasons for the occurrence of hydrates in the Shenhu area. However, most previous

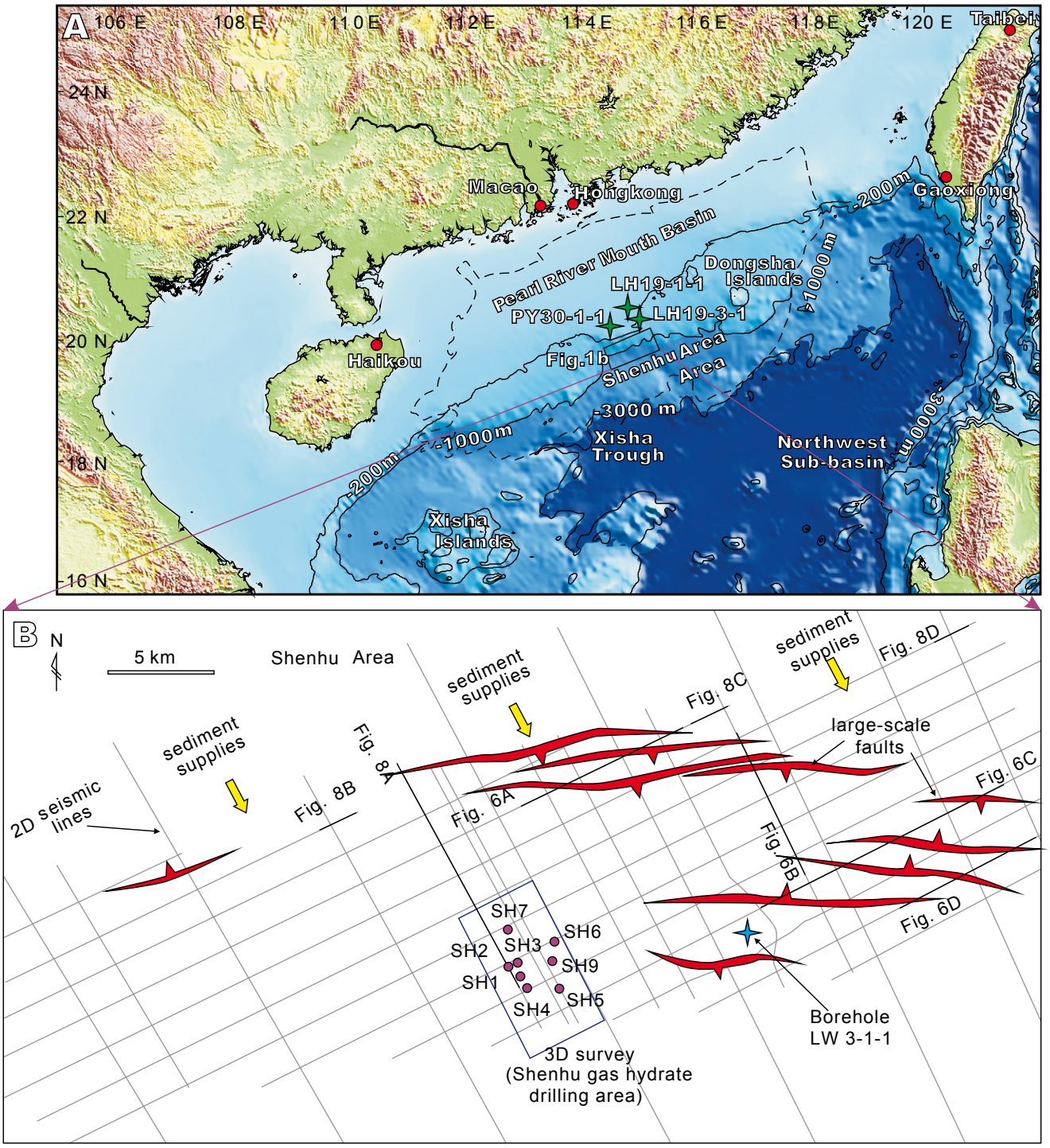

FIGURE 1. A) Shaded relief map of south China, showing the seafloor bathymetry of the northern continental slope of the South China Sea, and the locations of the Pearl River Mouth Basin (black dotted line) and the Shenhu area (black rectangle).Industrial boreholes used to analyze the contribution of thermogenic methane were displayed as green solid stars. B) Locations of the 2D seismic lines and 3D seismic survey used in this study. The violet rectangle highlighted the Shenhu gas hydrate drilling area, with the drill sites shown (circles). The nearby deep-water borehole LW3-1-1 (blue star) was also highlighted. Large-scale faults were shown in red. Yellow arrows marked the supposed sediment supplies from the North.

studies have focused on a single drilling site, especially the sites with hydrates (SH2 or SH7). Little attention has been given to the comparison between the eight sites, particularly those sites from which gas-hydrates were absent, which may result in some negligence of the regional outlook, and exaggeration the effect of the given factor on the formation and distribution of hydrates in this area.

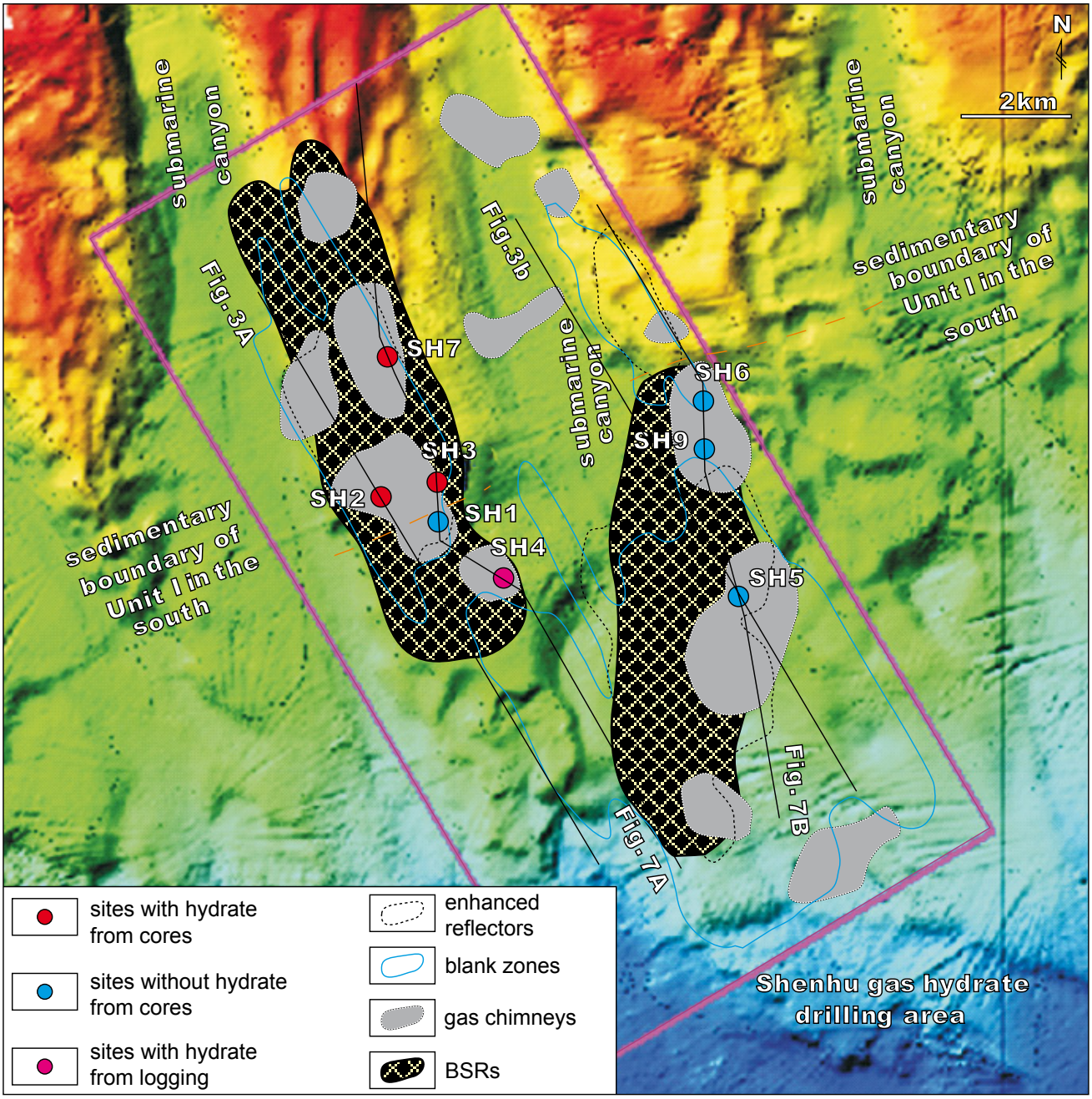

FIGURE 2. Topographic map of the gas hydrate drilling area showing the locations of the eight sites (pink rectangle). The distributions of BSRs, enhanced reflectors, blank zones and gas chimneys were illustrated. The orange dotted line marked the inferred sedimentary boundary of Unit I in the south. BSRs: bottom-simulating reflectors.

Therefore, the purposes of this study were: i) to characterize the variable distribution of gas hydrates which we have observed in the Shenhu area; ii) to describe the gas-hydrate petroleum system; iii) to reveal and document the distinctions between the eight sites through comparison and iv) to discuss impacts of the differences between the sites together with re-evaluation of previously proposed models. We integrated these results to better delineate the key factors that influence the accumulation and distribution of gas hydrates, which will improve our understanding of gas hydrate formation mechanisms in the Shenhu area, northern continental slope of the South China Sea.

GEOLOGICAL SETTING

The South China Sea (SCS) is one of the largest marginal seas in the western Pacific, located at the

intersection of the Eurasian, Indian-Australian, and Pacific plates. The northern continental slope of the SCS deepens to the southeast, with water depths increasing from 200m to 3000m into the Northwest Sub-basin (Fig. 1A). A series of gas hydrate investigations along the northern continental slope of the SCS have been carried out by GMGS since 1999. Many geological, geochemical, and geophysical characteristics associated with gas hydrates have been identified in the Qiongdongnan Basin, the Xisha Trough, the Pearl River Mouth Basin, and the Taixinan Basin, exhibiting a strong potential across the region (Guo *et al.*, 2004; Wang *et al.*, 2010; Wu *et al.*, 2005, 2007; Zhang *et al.*, 2002).

The Shenhu gas hydrate drilling area is located on the lower slope of the Baiyun Sag, Pearl River Mouth Basin, where abundant submarine canyons were developed (Fig. 2). The tectonic evolution of the Pearl River Mouth Basin conducted by Ru and Pigott (1986) suggested that the study area had undergone large tectonic subsidence since the Middle Miocene, probably related to the Dongsha and Taiwan tectonic activities (Yu *et al.*, 2012). Regional analyses shows the Baiyun Sag in particular had favourable geological conditions (water depths of 1000–1400m; seafloor pressures greater than 10MPa and seafloor temperatures below 4ºC) for gas hydrate formation (Zhang *et al.*, 2007). Lacustrine mudstones deposited during the Eocene were considered to be the thermogenic gas source (Huang *et al.*, 2003). Diapirs and faults served as migration pathways for gases/fluids (Chen *et al.*, 2013a; Qiao *et al.*, 2014; Su *et al.*, 2014a; Sun *et al.*, 2012a, b; Wu *et al.*, 2009) abyssal deposits in the shallow strata, such as turbidite channels, MTC, submarine fans, and contourites (Su *et al.*, 2013; Wang *et al.*, 2009).

MATERIALS

The high-resolution 2D and 3D seismic data analyzed in this study were collected by the ''FENDOU SI HAO'' of the GMGS between 2005 and 2006. The seismic data acquisition system consists of a 3-km, 240-channel streamer with 12.5m group spacing and a 160 cubic inch airgun array at a depth of 3m, giving full fold of 60. Sample rate is 1ms and record length is 6s. The dominant frequency of the data varies with depth but is approximately 60Hz at 1500m. 2D seismic lines were collected parallel or perpendicular to the shelf break in water depth from 200 to 3000m, covering the whole Shenhu area (Fig. 1B), helping to reveal the regional tectonic and sedimentary features.

The logging data as natural gamma-ray, gamma density, resistivity, and sonic velocity were acquired during the expedition. All the logging data at the eight sites have been reported by Wang *et al.* (2014b) to indicate the occurrences of hydrates in the Shenhu area. During GMGS-1, core samples were collected at SH1, SH2, SH3, SH5 and SH7 (Chen *et al.*, 2011, 2013b; Liu *et al.*, 2012; Wu *et al.*, 2008; Yang *et al.*, 2008) and illustrated the characteristics of grain size of the core samples. In this study, 116 samples, provided from GMGS, were collected at SH7 over depths from 0.1 to 176.7mbsf (meters below the seafloor) were used to generate Cm pattern (plotted one-percentile and median values from grain-size analyses), which could be used as evidence to identify the sedimentary units with different forming mechanisms proposed by Passega (1964).

DISTRIBUTION OF GAS HYDRATES IN THE SHENHU AREA

During the pre-drill analysis in the Shenhu area, several seismic anomalies were regarded as the indicators to infer the presence of hydrates, including BSRs, Enhanced Reflectors (ERs) and Blank Zones (BZs). Although some observations of BSRs on seismic profiles showed a smaller degree of gas hydrate in the sediments above the BSR (Wood and Ruppel, 2000; Holbrook *et al.*, 1996; MacKay *et al.*, 1994), they were still suggested to be the major geophysical indicator for the gas-hydrate occurrence (Berndt *et al.*, 2004; Haacke *et al.*, 2007; Shipley *et al.*, 1979). Across the drilling area, BSRs with reversed polarity could easily be identified parallel to the seafloor (Fig. 3) at varying depths of 170–242mbsf (Table 1), and were wide spread in the plane distribution (Fig. 2). Above BSRs, BZs are observed and might be caused by a reduction in impedance contrast from the hydrate-bearing strata, producing a sharp decrease in the seismic reflection amplitude; ERs below BSRs might be interpreted as free gas in the sediment pore space, which amplifies the energy of the seismic reflectors (Fig. 3). This BZ–BSR–ER model was considered to represent the typical geophysical pattern to predict the potential hydrates in the Shenhu area (Zhang *et al.*, 2012). Using this method, the spatial distribution of seismic features highlighted two zones with seismic anomalies, located at the ridges of the submarine canyons (Fig. 2), providing the reference basis for the drill site selection. For instance, BSRs, ERs, and BZs are all observed in the seismic profiles across SH2 and SH5 (Fig. 3).

However, of the eight drill sites, only SH2, SH3, and SH7 yielded hydrates in the recovered core samples (Fig. 2), with average saturations of 21.10%, 20.25%, and 23.09%, respectively (Wu *et al.*, 2008) (Table 1). During the expedition, hydrate-bearing samples were not recovered from SH1 and SH5. SH4, SH6, and SH9 were not sampled because they were considered to contain few or no hydrates according to the log data. Through the re-examination of log data at SH4, hydrates were inferred in thin-bedded sand-rich sediments with an

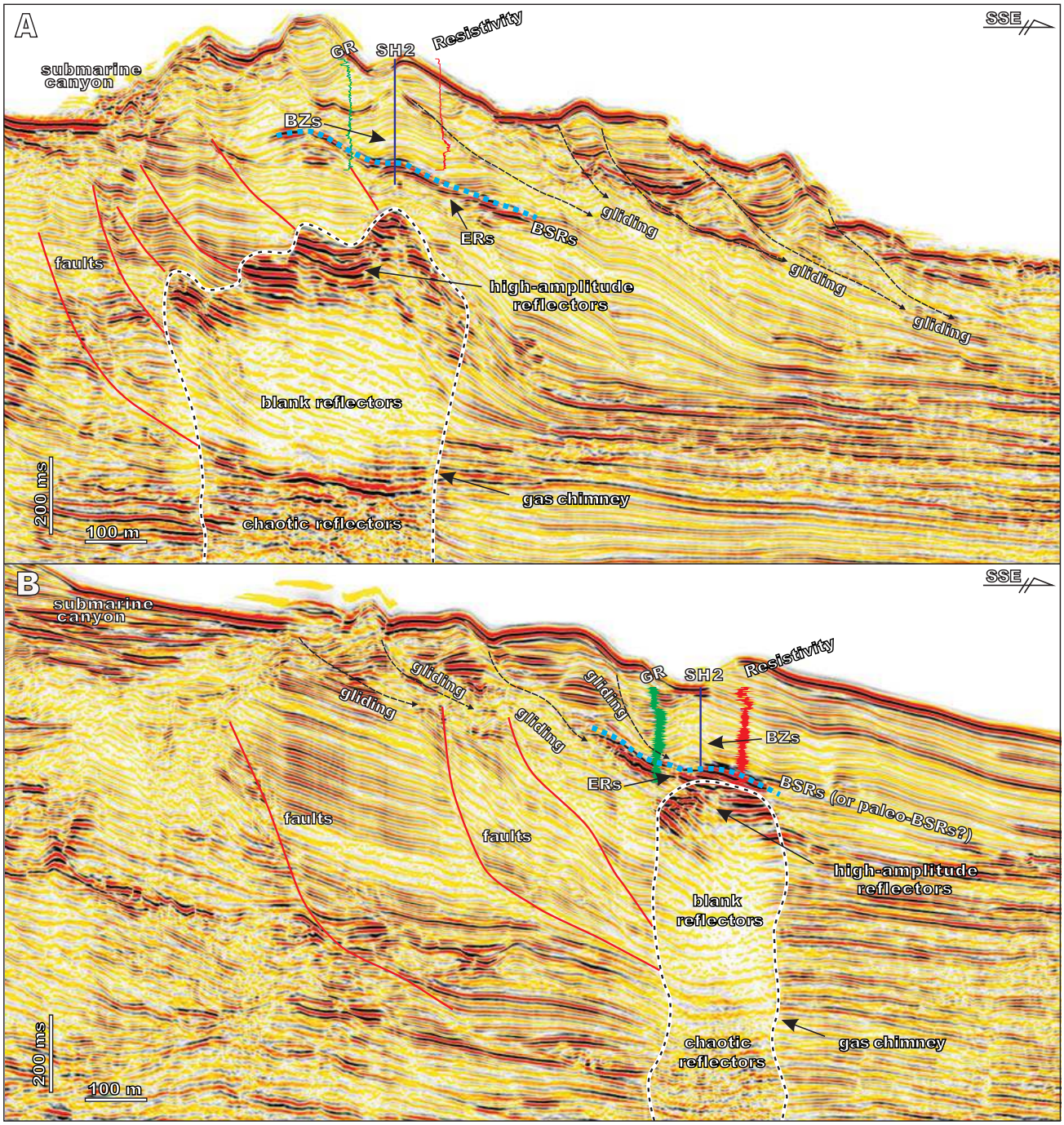

FIGURE 3. SSE-trending seismic profiles through A) SH2 and B) SH5 highlighting seismic anomalies (BSRs, ERs, and BZs), the logging curves (GR and resistivity), and the developments of gas chimneys and related faults. The drilling results revealed hydrates were recovered at SH2, with some anomaly values in the resistivity curve, corresponding to the BZs on the seismic profile. Due to the possible intrusion of late-stage mud diapir at SH5 (Li *et al.*, 2010; Wang *et al.*, 2010; Xu *et al.*, 2012), hydrates were dissociated completely, and BSRs might be the paleo-BSRs. Note some gliding features could be observed on the shallow sedimentary layers with some continuous reflectors. The locations of the seismic profiles were marked on Figure 2. BSRs: Bottom-Simulating Reflectors; ERs: Enhanced Reflectors; BZs: Blank Zones; GR: natural Gamma Ray.

average saturation of about 20% (Wang *et al.*, 2014a). That is to say, the GMGS-1 drilling campaign revealed a variable distribution of gas hydrates in the Shenhu area, covering an area of 15km^2 (Wu *et al.*, 2008). In plan-view, hydrates were only revealed at SH2, SH3 and SH7 from the recovered core samples, and conjectured through the log data at SH4 (Wang *et al.*, 2014a) (Fig. 2). Vertically, gas hydrates occurred in fine-grained deposits just above the base of Gas Hydrate Stability Zone (GHSZ) with a thickness of about 10–43m (Wu *et al.*, 2008; Yang *et al.*, 2008), where relatively high resistivity curves were also observed (Fig. 4). Taking the discontinuous core

TABLE 1. Basic parameters of the eight sites in the Shenhu gas hydrate drilling area. The water depths, seafloor temperatures, geothermal gradients, and the depths of base of BGHZ for each site were provided by GMGS. The seafloor pressures at the eight sites were calculated from the empirical formula of Kaul *et al.* (2000). Several seismic anomalies (BSRs, ERs, and BZs) were identified from the seismic profiles, which were used in the pre-drill analysis. The BSR depths for the eight sites were estimated from the geophysical data in the pre-drill analysis. Data on the average saturation of gas hydrates of SH2, SH3, and SH7 and the SMI depths at SH1, SH2, SH3, SH5, and SH7 are from Wu *et al.* (2011). The parameters at SH4 were cited from Wang *et al.* (2014a, 2014b). SMI: Sulfate-Methane Interface; mbsf: meters below sea floor; BSRs: Bottom-Simulating Reflectors; ER: Enhanced Reflectors; BZ: Blank Zones; BGHZ: Base of Gas Hydrate Zone

Site	Parameters				Pre-drill analysis		Drilling results		
	Water depth (m)	Seafloor temperature (°C)	Seafloor pressure (MPa)	Geothermal gradient (°C/km)	Seismic features	Depth of BSRs from geophysical data (mbsf)	Depth of the BGHZ (mbsf)	Average saturation of hydrates (%)	Depth of SMI (mbsf)
SH1	1262	5.21	12.78	47.53	BSRs, ER, and BZ	242	—	—	27.0
SH2	1230	4.84	12.46	46.95	BSRs, ER, and BZ	209	229	21.10	26.0
SH3	1245	5.53	12.61	49.34	BSRs, ER, and BZ	196	206	20.25	27.0
SH4	1290	—	13.06	—	BSRs, ER, and BZ	175	—	20.00	—
SH5	1423	4.72	14.40	67.60	BSRs, ER, and BZ	170	—	—	21.0
SH6	1217	—	12.33	—	BSRs, ER, and BZ	220	—	—	—
SH7	1105	6.44	11.20	43.65	BSRs, ER, and BZ	170	184	23.09	17.0
SH9	1265	—	12.81	—	BSRs, ER, and BZ	225	—	—	—

samples from SH2 as an example, the hydrate-bearing layer consists of silt and silty clays, with a silt content of 70%–80% and <2% sand (Chen *et al.*, 2011; Liu *et al.*, 2012). The Bases of Gas Hydrate Zone (BGHZ) were at about 229mbsf, 206mbsf, and 184mbsf at SH2, SH3, and SH7, respectively (Table 1).

GAS-HYDRATE PETROLEUM SYSTEM

Gas hydrate stability conditions

Regionally, the Baiyun Sag has been regarded as a suitable area for gas hydrates because of its water depth (1000–1400m), water pressure (>10MPa), and water temperature (<4ºC) (Zhang *et al.*, 2007) are favourable. These conditions provided further evidence for the drill site selection. The Shenhu gas hydrate drilling area is located at the lower slope of the Pearl Mouth River Basin (Fig. 1), at water depths of 1000–1500m. Furthermore, seafloor temperatures and pressures of about 3.38-4.58ºC and 10.15-15.17Mpa, respectively, were calculated through the temperature–depth relationship of Feng (1996) and the pressure–depth formula of Kaul *et al.* (2000). At all the eight sites, the seafloor temperatures and pressures display the basic conditions of low temperature and high pressure for hydrates (see Table 1). During the GMGS-1 drilling campaign, the geothermal gradient in the drilling area was about 43.65–67.60ºC/km, with the maximum value of 67.60°C/km at SH5 and the minimum value of 43.65ºC/km at SH7 (Table 1). These conditions, along with the observed seismic indicators, suggested that all the eight sites were suitable environment for the formation of gas hydrates (Table 2).

Gas composition and gas source

The study area is close to the deep-water borehole LW3-1-1 (blue solid star in Fig. 1B), the source rocks of which are primarily the Eocene Wenchang and Enping formations and Oligocene Zhuhai Formation (Zhu *et al.*, 2009). Thermogenic gases from a deep source were originally thought to be the main contributor of gas hydrates in the Shenhu area (Su *et al.*, 2011). However, geochemical analyses of pore water from the core samples revealed methane content of 96.10%–99.91% with small amounts of ethane and propane (Wu *et al.*, 2008). In particular, $\delta^{13}C_{CH4}$ values of headspace gases at SH2, SH3, and SH5 (–74.3‰ to –46.2‰) and the methane/ethane ratio above the hydrate-bearing layer (>1000) (Table 2) indicated that the methane forming gas hydrate was mainly produced biogenically or mixed methane dominated by microbial origin with a few contribution of thermogenic methane (Wu *et al.*, 2011; Zhu *et al.*, 2013). Through the C_1/C_{2+} ratios from void-gas samples, some features of thermogenic methane could be found at the drilling sites (Wang *et al.*, 2014b). Also, according to the geochemical analyses on industrial boreholes around the periphery of the Shenhu area (Hou *et al.*, 2008; Zhu *et al.*, 2009), characteristics of thermogenic methane can be found in the shallow strata. For instance, in the strata with depths of less than 1500m at Boreholes PY30-1-1, LH19-1-1, and LH19-3-1 (green solid stars in Fig. 1A), the values of $\delta^{13}C_{CH4}$ were higher than –45%, and the values of C_1/C_{2+} were much less than 1000 (Fig. 5). Therefore, it is difficult to classify the gas sources in the study area were originating only from biogenic gases. The

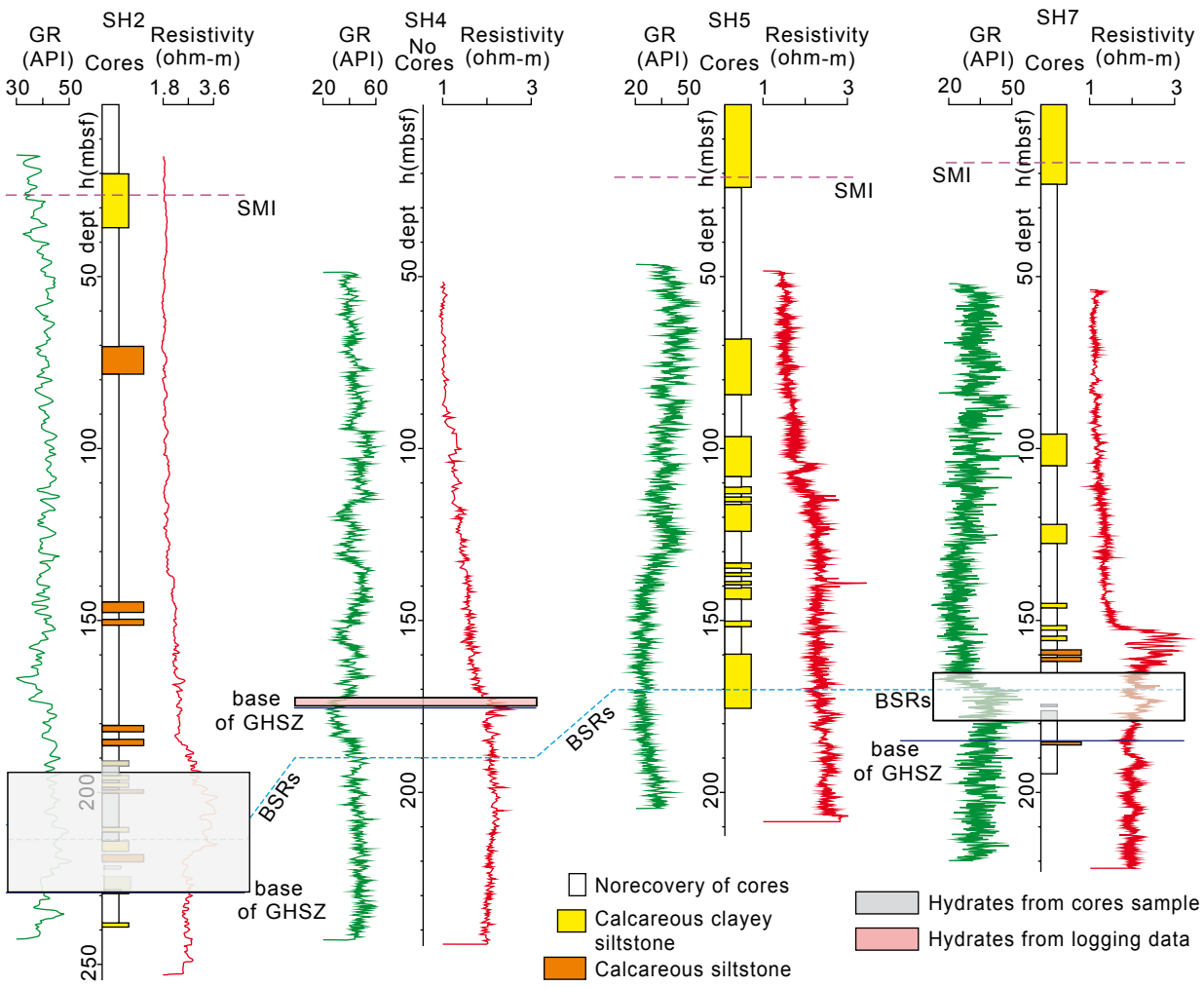

FIGURE 4. Summary core samples and logging curves at sites SH2, SH4, SH5 and SH7, showing the lithological features, and the depths of BSRs, the bases of GHSZ and SMI. Hydrates were documented from recovered core samples at SH2 and SH7. Thin-bedded hydrates accumulated in sand-rich sediments were proposed by Wang *et al.* (2014a). No hydrates were found at SH5. GR: natural Gamma Ray; mbsf: meters below seafloor; SMI: Sulfate-Methane Interface; GHSZ: Gas Hydrate Stability Zone; BSRs: Bottom-Simulating Reflectors.

contribution of thermogenic methane from deep source rocks is worth to be concerned. And in this study, we suggested that gas sources at all the eight sites might be mixed gases with dominated biogenic gases (Table 2).

Gas-bearing fluid migrations

In the Shenhu area, three types of migration pathways for gas-bearing fluids have been identified; faults; mud diapir and gas chimneys (Su *et al.*, 2014a). Seismic profiles (Fig. 6) indicate the development of WE/NE-trending faults in the northern and eastern Shenhu area (Fig. 1B). These faults extended downward to the Oligocene and Eocene strata and penetrated upward to the base of Late Miocene with some showing strip-shaped, chaotic reflectors (Fig. 6), implying the vertical migration of gases/fluids from deeper strata. However, these faults could not be observed in gas hydrate drilling area (Fig. 1B).

Through the seismic profiles crossing sites SH2 and SH5 (Fig. 3), gas chimneys could also be clearly identified by relatively steep anomalous reflectors potentially caused by the migration of gas-bearing fluids. Gas chimneys are commonly associated with the occurrence of gas hydrates (Haacke *et al.*, 2009; Horozal *et al.*, 2009; Riedel *et al.*, 2002) and thus were used along with BSRs for drill site selection (Fig. 2). The internal architecture of gas chimneys can be divided into three parts: chaotic reflectors at the bottom, a central zone of blank reflectors, and high-amplitude reflectors at the top (Fig. 3). Amplitude Versus Offset (AVO) analysis and instantaneous frequency analysis indicated the low-frequency anomaly over the centre of the gas

TABLE 2. Characteristics of the gas-hydrate petroleum system in the Shenhu drilling area highlighting the distinct differences between the eight sites. The geochemical results for SH2, SH3, SH5, and SH7 are adopted from Wu *et al.* (2011) and Zhu *et al.* (2013)

Site	Gas-hydrate petroleum system			
	Gas hydrate stability conditions	Gas composition and gas source	Gas-bearing fluids migration	Sedimentary conditions
SH1	water depth: 1262 m; seafloor temperature: 5.21 °C; seafloor pressure: 12.78 MPa; geothermal gradient: 47.53 °C/km	mixed gases with dominated biogenic gases	gas chimneys together with small-scale faults; low methane flux upwards	sedimentary Unit II;
SH2	water depth: 1230 m; seafloor temperature: 4.84 °C; seafloor pressure: 12.46 MPa; geothermal gradient: 46.95 °C/km	CH_4: 99.89%;$C_1/(C_2+C_3)$: 911.7;$\delta^{13}C_1$: -56.7%, PDB; mixed gases with dominated biogenic gases	gas chimneys together with small-scale faults; low methane flux upwards	sedimentary Unit II; sedimentary Unit I
SH3	water depth: 1245 m; seafloor temperature: 5.53 °C; seafloor pressure: 12.61 MPa; geothermal gradient: 49.34 °C/km	CH_4: 99.92%;$C_1/(C_2+C_3)$: 1373.5;$\delta^{13}C_1$: -61.6%, PDB mixed gases with dominated biogenic gases	gas chimneys together with small-scale faults; low methane flux upwards	sedimentary Unit II; sedimentary Unit I
SH4	water depth: 1290 m; seafloor pressure: 13.06 MPa;	mixed gases with dominated biogenic gases	gas chimneys together with small-scale faults; low methane flux upwards	sedimentary Unit II
SH5	water depth: 1423 m; seafloor temperature: 4.72 °C; seafloor pressure: 14.40 MPa; geothermal gradient: 67.60 °C/km	CH_4: 99.96%;$C_1/(C_2+C_3)$: 2447.0;$\delta^{13}C_1$: -54.1%, PDB mixed gases with dominated biogenic gases	gas chimneys together with small-scale faults; low methane flux upwards	sedimentary Unit II
SH6	water depth: 1217 m; seafloor pressure: 12.33 MPa;	mixed gases with dominated biogenic gases	gas chimneys together with small-scale faults; low methane flux upwards	sedimentary Unit II
SH7	water depth: 1105 m; seafloor temperature: 6.44 °C; seafloor pressure: 11.20 MPa; geothermal gradient: 43.65 °C/km	CH_4: 98.90%;$C_1/(C_2+C_3)$: 4200.6mixed gases with dominated biogenic gases	gas chimneys together with small-scale faults; low methane flux upwards	sedimentary Unit II; sedimentary Unit I
SH9	water depth: 1265 m; seafloor pressure: 12.81 MPa;	mixed gases with dominated biogenic gases	gas chimneys together with small-scale faults; low methane flux upwards	sedimentary Unit II

chimneys were caused by high seismic attenuation due to the vertical migration of gas-bearing fluids (Yang *et al.*, 2015). Gases/fluids might have migrated along chimneys upwards and into the GHSZ, causing the enrichment of free gas at the top of chimneys displayed as high-amplitude reflectors (Fig. 3). A number of small-scale faults were connected with chimneys, allowing the gas-bearing fluids to migrate more freely (Fig. 3). Additional micro-scale fractures developed within chimneys promoted gas-bearing fluids to migrate into GHSZ effectively (Sun *et al.*, 2012a, b; Yang *et al.*, 2015). Within GHSZ, hydrates may also accumulate within faults and fractures, as observed in the Ulleung Basin (Chun *et al.*, 2011). Hence, in the Shenhu gas hydrate drilling area, gas chimneys together with small-scale faults (or some micro-scale fractures) acted as the migration pathways for gases/fluids (Table 2), which were identified at all the eight sites.

Sedimentary conditions

Using the discontinuous recovered core samples, Chen *et al.* (2011) and Liu *et al.* (2012) reported that hydrate-bearing sediments were primarily composed of

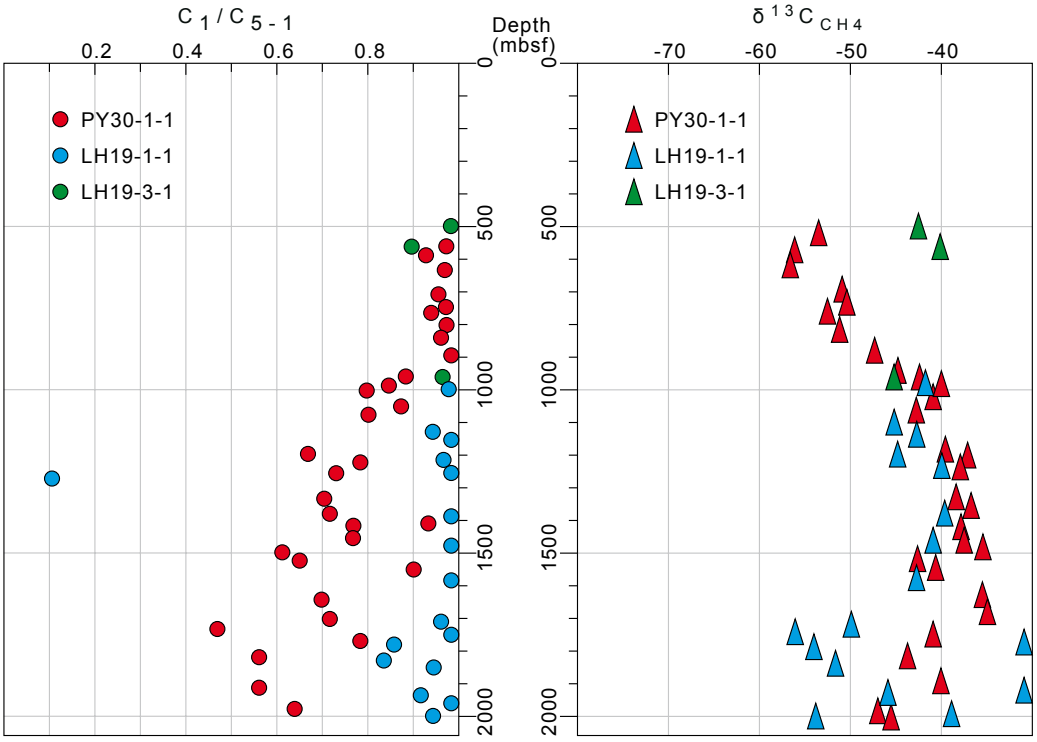

FIGURE 5. Geochemical analyses of $C_1/C_{1\text{-}5}$ and $\delta^{13}C_{CH4}$ from the industrial boreholes (PY30-1-1, LH19-1-1and LH19-3-1) near the Shenhu area illustrated that thermogenic gases/fluids may have migrated upwards into shallow strata with a depth of less than 1500m. The locations of boreholes were marked on Figure 1A.

fine-grained silt and silty clay predominated, which were similar to the surrounding sediments. However, in this study, we suggested for the first time two fine-grained sedimentary units with different forming mechanisms could be identified in the drilling area.

Unit I, fine-grained turbidites

Through the seismic profiles across the drilling sites, thin-bedded chaotic reflectors with lenticular/irregularly shaped geometries above BSRs could be observed (Fig. 7), located at the northern edge of the submarine canyon (Fig. 2). On the basis of sequence stratigraphic correlation and analyses of deep-water sedimentation (Su *et al.*, 2014b; also can see Fig. 8A in this report), sedimentary Unit I was proposed to be associated with small-scale deep-water channels developed in the North of the Shenhu area (Fig. 8). These small-scale deep-water channels showing U-shaped morphologies and obvious bases with widths of about 2–6km are visible on NEE-trending seismic profiles (Fig. 8B-D). The termination of the reflectors against the sides of such channels suggests that they were at some point erosional. The eroded materials (the underlying strata) were down-slope transported southwards, and re-deposited at the lower slope, at the hydrate drilling area.

From the Cm pattern at SH7 (Fig. 9), some distinct features could be found, helping the identification of the sedimentary Unit I. At site SH7, a total of 116 samples above the base of GHSZ (180mbsf in Table 1) at depths of about 0.1–176.7mbsf were collected to generate a reliable Cm pattern. 14 samples were taken at the depths between 155–176.7mbsf where hydrates were recovered, and the rest of the 102 samples ranged from depths of about 0.1–155mbsf. Graphing the Cm pattern revealed two groups of the samples. The first group (Group I), composed by the 13 samples, grouped together in a linear pattern parallel to the C=M baseline (Fig. 9). These samples where recognized as turbidites based on Passega (1964) classification system. By contrast, the other group (Group II) containing 102 samples showed different characteristics (Fig. 9).

Based on the grain size, seismic features, deep-water sedimentation analyses, and Cm pattern at SH7, the sedimentary Unit I at the bottom was interpreted as fine-grained turbidites. Chaotic reflectors associated with sedimentary Unit I could be interpreted and traced on seismic lines, at sites located in the North of the western and eastern ridges of the submarine canyon (such as SH3 and SH7 in Fig. 7A) suggesting that this unit extended right across the area around these sites as well as between

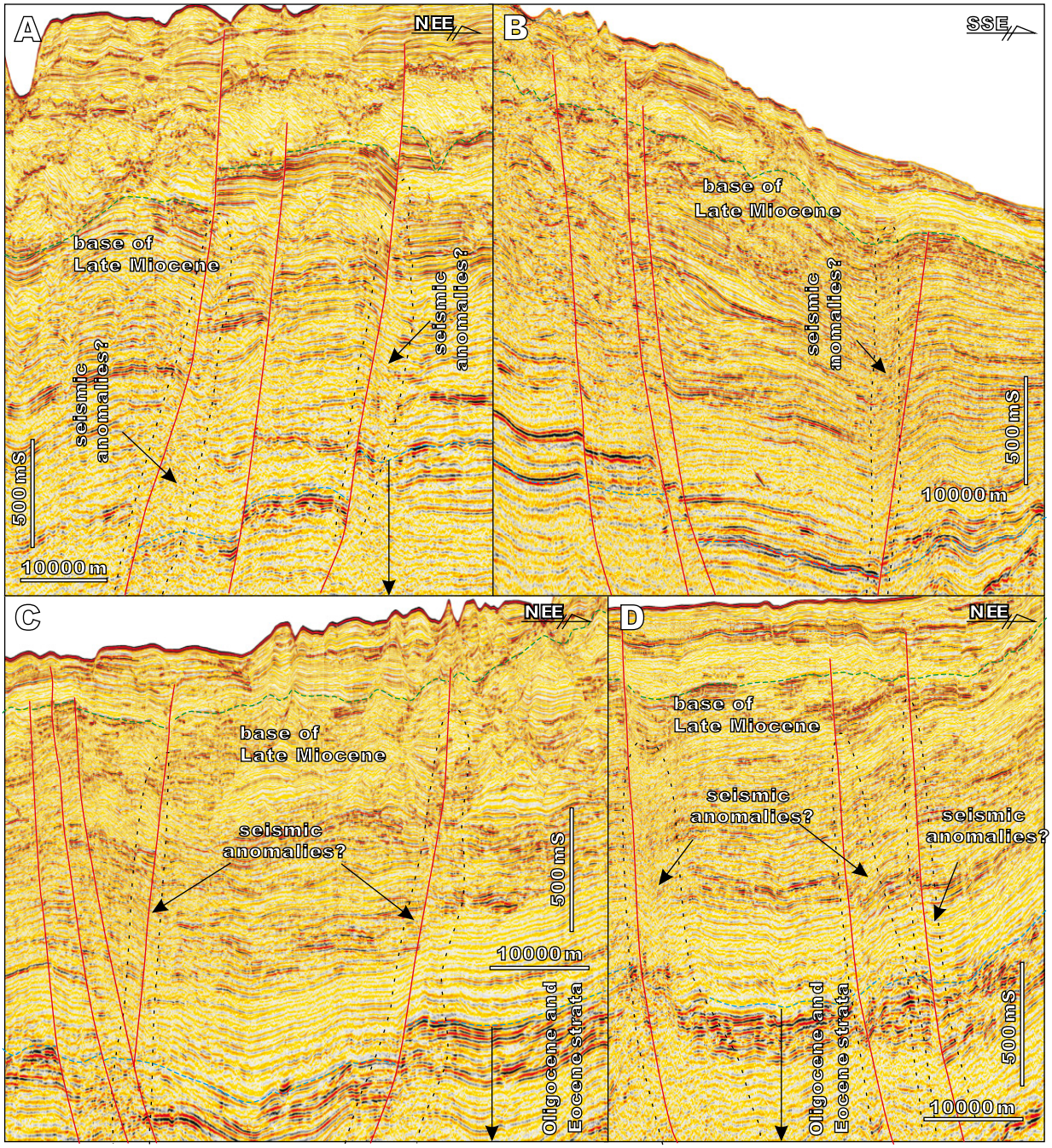

FIGURE 6. Characteristics of large-scale faults in the Shenhu area through the 2D seismic profiles. These faults, with WE/SEE orientations, are distributed in the North and Northeast of the Shenhu area and could not be observed in the gas hydrate drilling area (see Fig. 1B for the distributions). Some seismic anomalies related to these faults were attributed to be the vertical migrations of gases/fluids from the deep strata. The locations of the seismic profiles were marked on Figure 1B.

them. Site SH2 (located in the North of the ridge in Fig. 2) was also speculated to be located within the distribution of sedimentary Unit I, due to its close proximity to SH3 (300m, Fig. 2). As for the other sites, no evidence could be seen for the presence of sedimentary Unit I at sites SH1 and SH4 (Fig. 7A) at SH5, SH6, and SH9 (Fig. 7B).

Unit II, fine-grained sediments related to soft-sediment deformation

In the drilling area, the most common seismic characteristics above BSRs are continuous, moderate/high amplitude reflectors with spoon-shaped morphologies. These are widely developed on the both

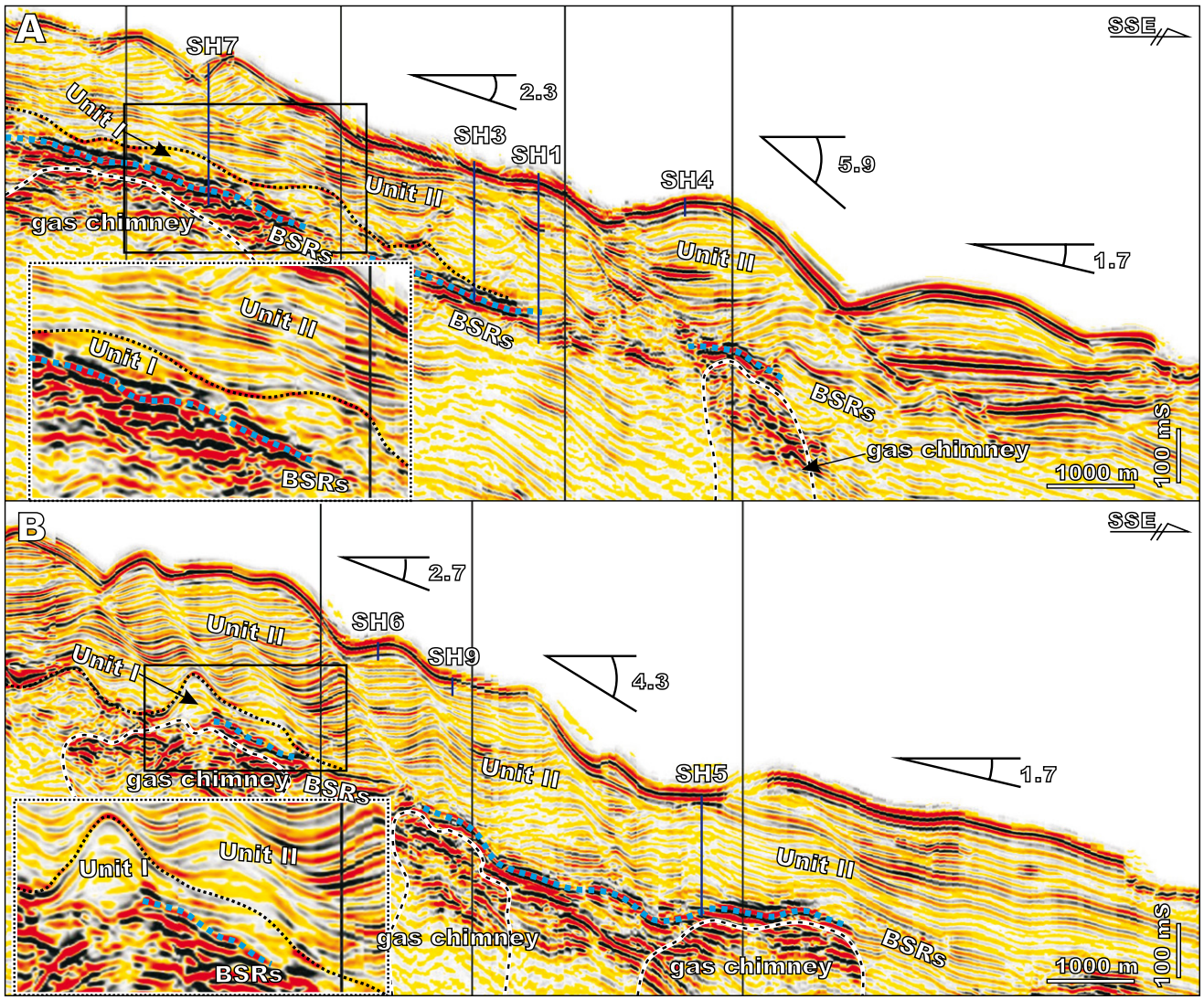

FIGURE 7. SSE-trending 3D seismic profiles across A) SH7, SH3, SH1 and SH4 and B) SH6, SH9 and SH5, showing the two sedimentary units above BSRs inferred from the seismic features. The thin-bedded sedimentary Unit I with chaotic reflectors developed on the bottom was represented as fine-grained turbidites associated with re-deposited sediments eroded by small-scale deep-water channels in the North. Overlying sedimentary Unit II with continuous reflectors was widely distributed, corresponding to fine-grained sediments related to soft-sediment deformation triggered by sufficient sediment inputs from the North and seafloor topographic features. The variations in slopes of these two profiles were calculated and labeled. Two locally enlarged profiles highlighted the characteristics of sedimentary Unit I. The locations of the seismic profiles were marked on Figure 2. BSRs: Bottom-Simulating Reflectors.

ridges of the submarine canyons (Figs. 3; 7). Along with similar log data patterns observed at SH5 and SH7 (Fig. 4) and fine-grained lithologies (Chen *et al.*, 2011; Liu *et al.*, 2012), these characteristics were described as another sedimentary unit, named herein sedimentary Unit II (Fig.7).

Within this unit, some offsets of seismic reflectors could be observed with general retention of the bedding identity (Figs. 3; 7), which had been interpreted as the submarine landslides (also called as slope failures) by He *et al.* (2014). Submarine landslides are the deposits of the down-slope movement of underconsolidated sediments as the result of gravitational forces, which usually result in the soft-sediment deformation of the transported material (Bull *et al.*, 2009; Hampton *et al.*, 1996; McAdoo *et al.*, 2000; Mills, 1983; Moscardelli and Wood, 2008). They are important processes on most continental margins and are one of the most important deep-water geomorphologic and depositional features in modern and ancient submarine successions (Hampton *et al.*, 1996; McAdoo *et al.*, 2000). Due to this method of transportation and deposition, coherent sections of material are commonly observed (*e.g.* Bull *et al.*, 2009), and are often referred to as blocks or slabs (Hüneke and Mulder, 2011).

Another interpretation of these continuous reflectors was sediment waves (Qiao *et al.*, 2015; Wang *et al.*, 2007; Wang *et al.*, 2014b), due to their asymmetric wavy characters and apparent upslope-wards migration of the internal architectures (Fig. 7). When present at the seafloor they procedure a relatively rough topographic character (Fig. 2). Many processes can produce wave-like structures, including bottom currents, turbidity currents and soft-sediment deformation (Wynn and Stow, 2002). In this study, these wavy structures were suggested to be the results of soft-sediment deformation. Firstly, sediment influx for the study area was sourced from the Pearl River drainage system in the North (Li *et al.*, 2003), due to its proximity and drainage catchment to the shelf and slope. Influenced by climate changes on erosion rates (Zhang *et al.*, 2001), exceptionally high sedimentation rates of Quaternary (10-30Km/Ky, Huang and Wang, 2006) observed in the Pearl River Mouth Basin might result in a sudden increase in under-consolidated sediments. The prograding features revealed through the SEE-trending profile (Fig. 8A) illustrate the high sediment inputs from the North (as yellow arrows in Fig. 1B). Secondly, the steeply dipping slopes in the Senhu area were described by Qiao *et al.* (2015) with slope of about 2º in average. Calculations of seafloor inclination on the riges of the submarine canyon (using acoustic velocity in seawater of about 1500m/s) show that dips at the North are 1.7º–5.9º and in the South are 1.7º–4.3º (Fig. 7). Such dips may increase the likely hood of soft-sediment deformation and slope failures. What is more, as reported by Wang *et al.* (2007), only the up slope-wards migrating features could be observed on the bathymetric map (Fig. 2) and seismic profiles (Fig. 7) in the study area, instead of evidences for lateral migrations.

Therefore, in the study area, whether the submarine landslides considered by He *et al.* (2014) wave-like structures suggested from Qiao *et al.* (2015), Wang *et al.* (2007) and Wang *et al.* (2014b) were underwent the same sedimentary process of soft-sediment deformation triggered by gravitational forces. In this report, the sedimentary Unit II at the top above BSRs with continuous reflectors was interpreted as the fine-grained sediments related to soft-sediment deformation.

DIFFERENCES BETWEEN THE EIGHT SITES THROUGH THE COMPARISONS

As described above on gas-hydrate petroleum system, the differences between the eight drilling sites in the Shenhu area are summarised in the comparisons table (Table 2) and concluded as three parts, including the seafloor temperatures and pressures related to the water depths, the geothermal gradient and the sedimentary conditions.

All the eight sites are located at a suitable temperatures (low) and pressures (high) for gas hydrates with minor variations in seafloor temperatures and pressures due to different water depths (Table 1). Geothermal gradients, determined during the GMGS-1, documented a locally higher geothermal gradient with a value of 67.6ºC/km at SH5, comparing to other sites with values of about 43.65–49.34ºC/km (Table 1).

Though the lithological characteristics of the discontinuous core samples were similar consisting of silt and silty clay (Fig. 4), two distinct sedimentary units above BSRs were identified. Fine-grained turbidites (Unit I) at the bottom and fine-grained sediments related to soft-sedimentary deformation (Unit II) at the top (Fig. 7). From the interpretations based on seismic profiles, sedimentary Unit I was only recovered at SH2, SH3 and SH7 (Fig. 7).

DISCUSSIONS: CONTROLLING FACTORS ON GAS HYDRATES OCCURRENCES AND DISTRIBUTIONS

Seafloor temperatures and pressures related to the water depths

Even though the water depths at the eight drill sites are different (from 1105m at SH7 to 1423m at SH5), which may lead to variations in the seafloor temperatures and pressures (Table 1), these conditions still provided a suitable environment (low temperature and high pressure) for the formation of hydrates. Using sites SH2 (with gas hydrates, water depth of 1230m, geothermal gradient of 46.95ºC/km), SH5 (without gas hydrates, water depth of 1423m, geothermal gradient of 67.60ºC/km), and SH7 (with gas hydrates, water depth of 1105m, geothermal gradient of 43.65ºC/km), along with the parameters cited from Su *et al.* (2012), the depths of the base of GHSZ at each site could be calculated from the methane-hydrate phase equilibrium curve (Sloan and Koh, 2008), yielding values of 221mbsf, 179mbsf, and 168mbsf, respectively (Fig. 10). These results could help to understand how variations in the thickness of the GHSZ at different sites correspond to water depths. However, only the changes in seafloor temperatures and pressures related to the water depths could not explain why hydrates were recovered at SH2 and SH7, rather than SH5.

Locally higher geothermal gradient

The northern continental margin of SCS was characterized as the relatively high heat flow values (He *et al.*, 2001; Shi *et al.*, 2003). In the Bainyun Sag, the heat flow values ranged 59–79mW/m^2 (Nissen *et al.*, 1995). Close to the drilling area, the measured result of the

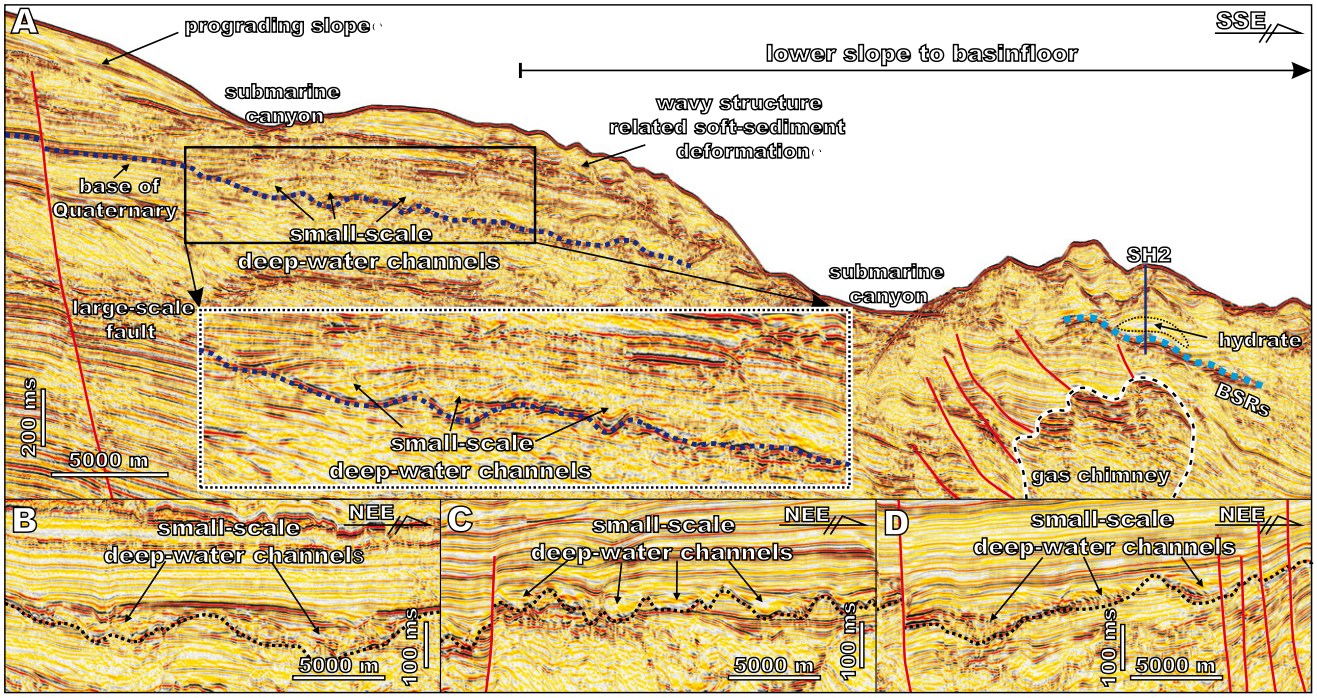

FIGURE 8. 2D seismic profiles displaying the features of the small-scale deep-water channels in the North of the Shenhu area. A) SSE-trending profile showing the stratigraphic correlations between small-scale deep-water channels in the North and the sedimentary Unit I (fine-grained turbidites) in the south. Also some prograding features indicating the sufficient sediment inputs were revealed. B-D) Three NEE-trending profiles displaying the features of small-scale deep-water channels in the northern Shenhu area with widths of about 2–6km. See Figure 1B for the locations. BSRs: Bottom-Simulating Reflectors.

industrial Borehole LW3-1-1 (blue solid star in Fig. 1B) was about 92mW/m^2 (Yuan *et al.*, 2009). In-suit heat flow measurements in the deep-water area of the northern slope of SCS showed the values in the Shenhu area were about 56–101mW/m^2 (Li *et al.*, 2010). During GMGS-1, the heat flow values at SH1, SH2, SH3, SH4 and SH7 in the western ridge were less than 76mW/m^2, whereas, the values at SH5, SH6 and SH9 in the eastern ridge were more than 80mW/m^2 (Wang *et al.*, 2010).

At site SH5, the relatively higher heat flow value was coincident with the locally higher geothermal gradient of about 67.60ºC/km (Table 1). Wang *et al.* (2010) suggested the seismic anomalies (gas chimney shown in this report) below BSRs on profile crossing SH5 (Fig. 3B) might be represent the intrusion of late-stage mud diapir, leading to the relatively higher geothermal gradient and heat flow. At this site, hydrates were thought to be dissociated completely, which may be the reason why no gas hydrates have been recovered (Li *et al.*, 2010; Wang *et al.*, 2010; Xu *et al.*, 2012).

Obviously, locally anomalous heat flow and geothermal gradient would have great effects on changing the thickness of GHSZ (Ganguly *et al.*, 2000; Kaul *et al.*, 2000; Shankar and Riedel, 2010; Shedd *et al.*, 2012), as shown in Figure 10. However, it is hard to clarify that no hydrates recovered at SH5 were attributed to entire dissociation due to a possible mud diaper (Fig. 3B). Until now, very few pieces of evidences through bathymetric and seismic data (Fig. 2; 3B; 7B) could be used to directly support this hypothesis, such as venting, pockmarks, local stratigraphic disturbance, collapses and so on.

Two distinct sedimentary units above BSRs

Porosity and permeability are two major parameters that can be used to characterize the physical property of sediments. Usually, porosity can be determined through the analyses of log data or measured directly from core samples. Grain size and sorting can also be used as an indicator of porosity, however it is largely indirect as for a given grain-size and sorting the associated porosity is also dependent on compaction and diagenesis during burial. In the Shenhu drilling area, the grain sizes were measured from the collected core samples at SH2, SH3, SH5 and SH7 (Chen *et al.*, 2011; Liu *et al.*, 2012), and were composed of fine-grained silt and silty clay. Permeability from core samples was not measured nor reported in literature. Despite grain sizes and lithological features for core samples with or without hydrates appeared to be similar, it does not mean the sediments of two distinct units above BSRs are homogeneousness.

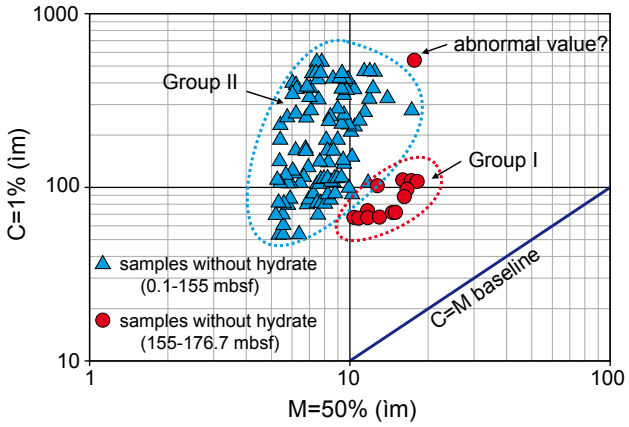

FIGURE 9. Cm pattern at site SH7 with totally 116 samples above the base of GHSZ within the depths of about 0.1–176.7mbsf. Among them, 13 samples (Group I) with hydrates at the depths between 155–176.7mbsf are paralleling to the C=M baseline with one abnormal value, indicating sedimentary Unit I might be turbidites as suggested by Passega (1964). And the rest 102 samples (Group II) without hydrates at the depths between 0.1–155mbsf show different features. GHSZ: Gas Hydrate Stability Zone; mbsf: meters below seafloor.

In the deep-water setting, the physical property of sediments (or reservoir quality) would be dependent on large variety of factors, including grain size, depositional process, depositional environment, sediment source and maturity (Shanmugam, 2006). Due to the lack of analyses on permeability of core samples, in this report, a preliminary discussion on the physical properties of the two sedimentary units on the basis of different forming mechanisms and sedimentary processes was given only.

Deep-water turbidites are attractive reservoirs in deep-water oil/gas explorations due to their relatively good reservoir qualities (Walker, 1978; Hüneke and Mulder, 2011; Khain and Polyakova, 2004; Stow and Mayall, 2000; Weimer and Roger, 2004). For marine gas hydrates, turbidites have been reported as the good host rocks, especially the buried channels and levee systems, as documented in the northern Cascadia (Torres *et al.*, 2008), the Krishna–Godavari Basin (Riedel *et al.*, 2011), the Gulf of Mexico (Boswell *et al.*, 2012a, 2012b), the Nankai Trough (Noguchi *et al.*, 2011; Ito *et al.*, 2015), the Ulleung Basin (Riedel *et al.*, 2013a, 2013b), the offshore of Taiwan (Lin *et al.*, 2014), and the northern South China Sea (Yu *et al.*, 2014).

In contrast, underconsolidated fine-grained sediments in the deep-water environment would maximize the occurrence of deformation especially when associated with areas or times of high depositional rate, low permeability, and low shear strength of grains (Mills, 1983; Van Loon and Brodzikowski, 1987). That is to say, relative sea level changes, erosional gravity flows, seafloor topographic features, tectonic activities, earthquake, bioturbation, gas expulsion, and other factors might lead to soft-sediment deformation on the continental slopes. The primary mechanisms responsible for soft-sediment deformation include liquefaction or fluidization, reverse density gradation, gravitational slump, and shear stress (Mills, 1983). Commonly, all these four processes could exist during the development of soft-sediment deformation. Due to the flow of liquefied sediments, the content of mud matrix would be increased as reported in the eastern side of the Monterey Canyon (Normark *et al.*, 1985). Moreover, creep would be a long-term deformation process of sediments submitted to a constant load on slope with relatively low velocity of deformation (Shanmugam, 2006; Hüneke and Mulder, 2011; Mulder and Cochonat, 1996), which also result in the enhancement of contact degree between particles. Thus, fine-grained soft-sediment deformation generally is not considered to be good reservoirs (Shanmugam, 2006).

Compared to the fine-grained turbidites identified at the bottom (Fig. 7), the higher content of mud in the matrix and relatively high contact degree between particles might have occurred in the fine-grained sediments related to soft-sediment deformation. As a consequence, in this report, we proposed that, although the lithology and grain size of the hydrate-bearing sediments were similar to the other sediments, as silt and silty clay predominated (Chen *et al.*, 2011; Liu *et al.*, 2012), the distinct two units associated

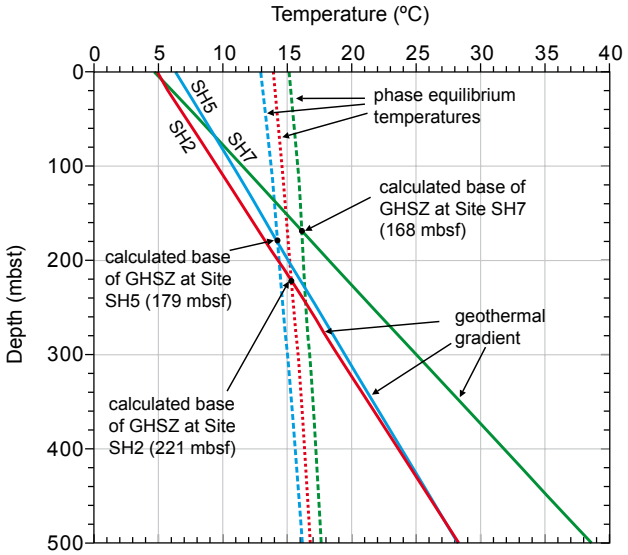

FIGURE 10. Calculated base of the GHSZ at sites SH2, SH5, and SH7 using the methane-hydrate phase equilibrium curve (Sloan and Koh, 2008). The red solid line and dotted line represent the phase equilibrium temperature and geothermal gradient of SH2, respectively. The blue solid line and dotted line represent the phase equilibrium temperature and geothermal gradient of SH5, respectively. The green solid line and dotted line represent the phase equilibrium temperature and geothermal gradient of SH7, respectively. mbsf: meters below seafloor; GHSZ: Gas Hydrate Stability Zone.

with different formation mechanisms and sedimentary processes implied sedimentary conditions above BSRs in the drilling area varied over time and space (Figs. 2; 3; 7). As for the physical properties of sediments, fine-grained turbidites were preferred to be better host rocks than fine-grained deformed sediments. So, sedimentary Unit I characterised by thin-bedded chaotic reflectors are proposed as host rocks for hydrates; whereas the overlying unit, sedimentary Unit II characterised by thick continuous reflectors, would serve as regional homogeneous caprocks.

Possible model

Besides suitable hydrate stability conditions (low temperatures and high pressures) and potential gas sources (biogenic and thermogenic origins), some workers have pointed out that the migration of gas-bearing fluids and the occurrence of favourable sediments would play important roles in the formation and presence of marine gas hydrates (Collett *et al.*, 2009; Tréhu *et al.*, 2006; Yu *et al.*, 2014). In the Shenhu gas hydrate drilling area, all the eight sites were located in an environment of suitable seafloor temperatures and pressures of about 3.38–4.58ºC and 10.15–15.17MPa (Table 1). The variations of seafloor temperatures and pressures related to water depths and geothermal gradients between the eight sites would lead to the changes in the thickness of GHSZ (Fig. 10). Biogenic and thermogenic gases were contributed to formation of hydrates in the study area (Table 2). Gas chimneys together with faults (or some micro-scale fractures) composed the migrating pathways for gas-bearing fluids (Table 2), which the chimney structures could be observed at all the eight sites (Figs. 3; 7). The relatively deep Sulfate-Methane Interface (SMI) varying from 17mbsf to 27mbsf at SH1, SH2, SH3, SH5 and SH7 (Table 1), as an indicator for methane flux (Borowski *et al.*, 1996), implied the regional relatively low upward methane flux (Wu *et al.*, 2011). Between the sites with hydrates and the sites without hydrates, development and distribution of the two sedimentary units above BSRs (Fig. 7; Table 2) should be paid more attentions.

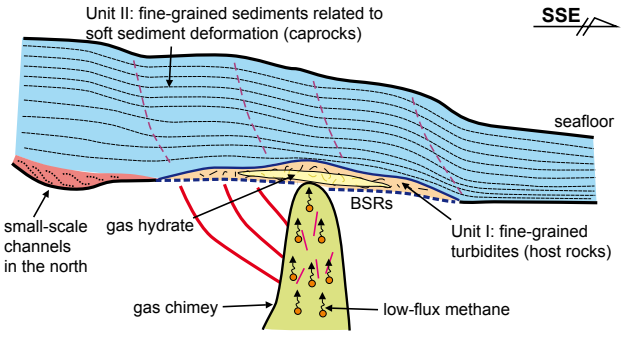

FIGURE 11. Cartoon of the possible model for the formation and occurrence of hydrates in the Shenhu drilling area, northern continental slope of the South China Sea. Around gas chimney, the small-scale faults and micro-scale fractures were represented as the red and magenta lines, respectively. BSRs: Bottom-Simulating Reflectors.

Herein, the proposed model suggests that the depositional processes of the sedimentary units are the crucial controlling factor for formation and occurrence of hydrates in the Shenhu drilling area. Low-flux methane could have migrated upwards through gas chimneys and entered into sedimentary Unit I (fine-grained turbidites) within GHSZ, causing the concentration of methane to exceed its solubility and thereby resulting in the formation of hydrates (Fig. 11). The overlying sedimentary Unit II (fine-grained sediments related to soft-sediment deformation) would be regarded as a compact layer with continuous reflectors hindered the further vertical migrations of gas-bearing fluids, sealing hydrates in the underlying sedimentary Unit I (Fig. 11). Also, the occurrences of hydrates within fine-grained turbidites (Unit I) would impede the upwards migrating of gases/fluids. The reason that no hydrates were recovered in Unit II within GHSZ was probably due to the extremely low methane concentration in this sedimentary unit.

This possible model could be used to explain the variable distribution of hydrates in the drilling area. Vertically, gas hydrates might only occur within fine-grained turbidites which would explain why hydrates were recovered within the sediments just above the base of GHSZ (Fig. 4), such as about 10–40m thick hydrate-bearing layers at SH2, SH3, and SH7(Wu *et al.*, 2008; Yang *et al.*, 2008). Through the seismic profiles (Fig. 7), the sedimentary boundary of fine-grained turbidites in the south could be traced on the bathymetric map (orange dotted line in Fig. 2), indicating is varying distribution. All the sites with hydrates from the recovered core samples (SH2, SH3 and SH7) were located within the area of sedimentary Unit I (Figs. 2; 7A), whereas, sites SH1, SH4, SH5, SH6 and SH9 absent of hydrates were located in the area with only fine-grained sediments related to soft-sediment deformation (sedimentary Unit II) (Figs. 2; 7B).

Additionally, about 17 submarine canyons were developed in Shenhu area as previously reported by Ding *et al.* (2013), Gong *et al.* (2013), Li *et al.* (2013); Lv *et al.* (2012) and Zhu *et al.* (2010). At the present day, the fine-grained turbidites (Unit I) might be only preserved as patches in the North of the canyon ridges (Fig. 2), where the hydrate-bearing sites SH2, SH3, and SH7 are located. The erosion and sedimentation of submarine canyons might cause the dissociation of hydrates as reported in the Mauritanian continental slope (Davies *et al.*, 2012).

CONCLUSIONS

We used a joint analysis of the seismic features revealed during the pre-drill analysis and the drilling results of the GMGS-1 in 2007 to characterize the variable distribution of gas hydrates in the Shenhu area, northern continental slope of the SCS. The factors of gas-hydrate petroleum system have been described in the study area and the distinct differences between the eight sites have been revealed. The conclusions are as follows:

i) During the pre-drill analysis, two zones of seismic anomalies (BSRs, ERs, and BZs) could be identified, which are located along the ridges of the submarine canyon. However, the drilling results revealed that gas hydrates were only present along western ridge, accumulating in fine-grained deposits with thicknesses of about 10m to 40m above the base of GHSZ, highlighting a variable gas hydrate distribution.

ii) The water depths, seafloor temperatures and seafloor pressures in the study area are favourable for gas hydrate formation. The methane content is about 96.10%–99.91%, with a small amount of ethane, which was thought to be mixed-sources gas. Gas chimneys and small-scale faults provide the migration pathways for the gas-bearing fluids with low upwards flux. Though the sediments above BSRs are similar in grain size and lithological feature, two sedimentary units could be identified; fine-grained turbidites at the bottom and fine-grained sediments related to soft-sediment deformation overlying at the top. On the basis of the analyses focused on sedimentary processes and sedimentary environments, these two fine-grained units were suggested to be different in the physical properties, fine-grained turbidites were preferred to be better than fine-grained sediments related to soft-sediment deformation.

iii) By comparing the eight sites, the sedimentary conditions are proposed to be the critical controlling factor for the accumulation and distribution of hydrates in the study area. Sedimentary Unit I with chaotic reflectors interpreted as fine-grained turbidites could serve as the host rocks for hydrates, whereas sedimentary Unit II, fine-grained sediments related to soft-sediment deformation, with continuous reflectors might act as a regional caprocks hindering the migration of gas-bearing fluids. The distribution of sedimentary Unit I might be the pivotal issue for the variable distribution of gas hydrates in the Shenhu drilling area, northern continental slope of the SCS.

ACKNOWLEDGMENTS

This study was supported by the National Natural Science Foundation of China (No. 41202080), the Open Fund of State Key Laboratory of Oil and Gas Reservoir Geology and Exploitation (Chengdu University of Technology) (No. PLC201402), and the PetroChina Innovation Foundation (No. 2013D-5006-0105). We would like to thank Luke Fairweather, Zheng Su, Daidai Wu, Hui Zhang, and Cuimei Zhang for their valuable discussions and helpful suggestions. We are very grateful to the journal editor and two anonymous reviewers for their critical reviews and constructive comments.

REFERENCES

Berndt, C., Bünz, S., Clayton, T., Mienert, J., Saunders, M., 2004. Seismic character of bottom simulating reflectors: examples from the mid-Norwegian margin. Marine and Petroleum Geology, 21(6), 723-733. DOI: 10.1016/j.marpetgeo.2004.02.003

Borowski, W.S., Paull, C.K., Ussler, W., 1996. Marine pore-water sulfate profiles indicate in situ methane flux from underlying gas hydrate. Geology, 24(7), 655-658. DOI: 10.1130/0091-7613(1996)024<0655:MPWSPI>2.3.CO;2

Boswell, R., Frye, M., Shelander, D., Shedd, W., McConnell, D.R., Cook, A., 2012a. Architecture of gas-hydrate-bearing sands from Walker Ridge 313, Green canyon 955, and Alaminos canyon 21: northern deepwater Gulf of Mexico. Marine and Petroleum Geology, 34(1), 134-149. DOI: 10.1016/j.marpetgeo.2011.08.010

Boswell, R., Collett, T.S., Frye, M., Shedd, W., McConnell, D.R., Shelander, D., 2012b. Subsurface gas hydrates in the northern Gulf of Mexico. Marine and Petroleum Geology, 34(1), 4-30. DOI: 10.1016/j.marpetgeo.2011.10.003

Bull, S., Cartwright, J., Huuse, M., 2009. A review of kinematic indicators from mass-transport complexes using 3D seismic data. Marine and Petroleum. Geology, 26(1), 1132-1151. DOI: 10.1016/j.marpetgeo.2008.09.011

Chen, D.X., Wu, S.G., Dong, D.D., Mi, L.J., Fu, S.Y., Shi, H.S., 2013a. Focused fluid flow in the Baiyun Sag, northern South China Sea: implications for the source of gas in hydrate reservoirs. Chinese Journal of Oceanology and Limnology, 31, 178-189. DOI: 10.1007/s00343-013-2075-5

Chen, F., Zhou, Y., Su, X., Liu, G.H., Lu, H.F., Wang, J.L., 2011. Gas hydrate saturation and its relation with grain size of the hydrate-bearing sediments in the Shenhu Area of northern South China Sea (in Chinese with English abstract). Marine Geology & Quaternary Geology, 31(5), 95-100. DOI: 10.3724/SP.J.1140.2011.05095

Chen, F., Su, X., Lu, H.F., Zhou, Y., Zhuang, C., 2013b. Relations between biogenic component (foraminifera) and highly saturated gas hydrates distribution from Shenhu Area, northern South China Sea (in Chinese with English abstract). Earth Science—Journal of China University of Geosciences, 38, 907-915.

Chun, J.H., Ryu, B.J., Son, B.K., Kim, J.H., Lee, J.Y., Bahk, J.J., Kim, H.J., Woo, K.S., Nehza, O., 2011. Sediment mounds and other sedimentary features related to

hydrate occurrences in a columnar seismic blanking zone of the Ulleung Basin, East Sea, Korea. Marine and Petroleum Geology, 28(10), 1787-1800. DOI: 10.1016/j.marpetgeo.2011.06.006

Collett, T.S., 2002. Energy resource potential of natural gas hydrates. American Association of Petroleum Geologists Bulletin, 86(11), 1971-1992. DOI: 10.1306/61EEDDD2-173E-11D7-8645000102C1865D

Collett, T.S., 2009. Gas hydrate petroleum systems in marine and Arctic permafrost environments. Houston (Texas, USA), 29th Annual Gulf Coast Section of Society for Sedimentary Geology (GCSSEPM Foundation Bob F. Perkins Research Conference December 2009, 6-8.

Collett, T.S., Johnson, A., Knapp, C., Boswell, R., 2009. Natural gas hydrates: energy resource potential and associated geologic hazards. American Association of Petroleum Geologists, 89 (Memoir), 781pp. ISBN: 0891813705

Colwell, F., Matsumoto, R., Reed, D., 2004. A review of the gas hydrates, geology, and biology of the Nankai Trough. Chemical Geology, 205(3.4), 391-404. DOI: 10.1016/j.chemgeo.2003.12.023

Davies, R.J., Thatcher, K.E., Mathias, S.A., Yang, J.X., 2012. Deepwater canyons: an escape route for methane sealed by methane hydrate. Earth and Planetary Science Letters, 323-324, 72-78. DOI: 10.1016/j.epsl.2011.11.007

Dickens, G.R., 2003. Rethinking the global carbon cycle with a large, dynamic and microbially mediated gas hydrate capacitor. Earth and Planetary Science Letters, 213(3-4), 169-183. DOI: 10.1016/S0012-821X(03)00325-X

Dickens, G.R., O'Neil, J.R., Rea, D.K., Owen, R.M., 1995. Dissociation of oceanic methane hydrate as a cause of the carbon isotope excursion at the end of the Paleocene. Paleoceanography, 10(6), 965-971. DOI: 10.1029/95PA02087

Ding, W.W., Li, J.B., Li, J., Fang, Y.Z., Tang, Y., 2013. Morphotectonics and evolutionary controls on the Pearl River Canyon system, South China Sea. Marine Geophysical Researches, 34(3), 221-238. DOI: 10.1007/s11001-013-9173-9

Ganguly, N., Spence, G.D., Chapman, N.R., Hyndman, R.D., 2000. Heat flow variations from bottom simulating reflectors on the Cascadia margin. Marine Geology, 164(1-2), 53-68. DOI: 10.1016/S0025-3227(99)00126-7

Gong, C.L., Wang, Y.M., Zhu, W.L., Li, W.G., Xu, Q., 2013. Upper Miocene to Quaternary unidirectionally migrating deep-water channels in the Pearl River Mouth Basin, northern South China Sea. American Association of Petroleum Geologists Bulletin, 97(2), 285-308. DOI: 10.1306/07121211159

Guo, T.M., Wu, B.H., Zhu, Y.H., Fan, S.S., Chen, G.J., 2004. A review on the gas hydrate research in China. Journal of Petroleum Science and Engineering, 41(1-3), 11-20. DOI: 10.1016/S0920-4105(03)00139-6

Haacke, R.R., Westbrook, G.K., Hyndman, R.D., 2007. Gas hydrate, fluid flow and free gas: formation of the bottom-simulating reflector. Earth and Planetary Science Letters, 261(3-4), 407-420. DOI: 10.1016/j.epsl.2007.07.008

Haacke, R.R., Hyndman, R.D., Park, K.P., Yoo, D.G., Stoian, I., Schmidt, U., 2009. Migration and venting of deep gases into the ocean through hydrate-choked chimneys offshore Korea. Geology, 37(6), 531-534. DOI: 10.1130/G25681A.1

Hampton, M.A., Lee, H.J., Locat, J., 1996. Submarine landslides. Reviews of Geophysics, 34(1), 33-59. DOI: 10.1029/95RG03287

He, L.J., Wang, K.L., Xiong, L.P., Wang, J.Y., 2001. Heat flow and thermal history of the South China Sea. Physics of the Earth and Planetary Interiors, 126(3-4), 211-220. DOI: 10.1016/S0031-9201(01)00256-4

He, Y., Zhang, G.F., Wang, L.L., Kuang, Z.G., 2014. Characteristics and occurrence of submarine canyon-associated landslides in the middle of the northern continental slope, South China Sea. Marine and Petroleum Geology, 57, 546-560. DOI: 10.1016/j.marpetgeo.2014.07.003

Hesse, R., 2003. Pore water anomalies of submarine gas-hydrate zones as tool to assess hydrate abundance and distribution in the subsurface: What have we learned in the past decade? Earth-Science Reviews, 61(1-2), 149-179. DOI: 10.1016/S0012-8252(02)00117-4

Holbrook, W.S., Hoskins, H., Wood, W.T., Stephen, R.A., Lizarralde, D., 1996. Methane hydrate and free gas on the blake ridge from vertical seismic profiling. Science, 273(5283), 1840-1843. DOI: 10.1126/science.273.5283.1840

Horozal, S., Lee, G.H., Yi, B.Y., Yoo, D.G., Parl, K.P., Lee, H.Y., Kim, W., Kim, H.J., Lee, K., 2009. Seismic indicators of gas hydrate and associated gas in the Ulleung Basin, East Sea (Japan Sea) and implications of heat flows derived from depths of the bottom-simulating reflector. Marine Geology, 258(1-4), 126-138. DOI: 10.1016/j.margeo.2008.12.004

Hou, D.J., Pang, X., Xiao, J.X., Zhang, J.C., Shi, H.S., Wang, J.R., Shu, Y., Zu, J.Z., 2008. Geological and geochemical evidence on the identification of natural gas migration through fault system, Baiyun Sag, Pearl River Mouth Basin, China. Earth Science Frontiers, 15(4), 81-87. DOI: 10.1016/S1872-5791(08)60041-X

Huang, W., Wang, P.X., 2006. Sediment mass and distribution in the South China Sea since the Oligocene. Science in China Series D: Earth Sciences, 49(11), 1147-1155. DOI: 10.1007/s11430-006-2019-4

Huang, B.J., Xiao, X.M., Zhang, M.Q., 2003. Geochemistry, grouping and origins of crude oils in the Western Pearl River Mouth basin, offshore South China Sea. Organic Geochemistry, 34(7), 993-1008. DOI: 10.1016/S0146-6380(03)00035-4

Hüneke, H., Mulder, T., 2011. Deep-sea sediments. Developments in Sedimentology, 63. Amsterdam, Elsevier, 849pp. ISBN: 9780444530004

Ito, T., Komatsu, Y., Fujii, T., Suzuki, K., Egawa, K., Nakatsuka, Y., Konno, Y., Yoneda, J., Jin, Y., Kida, M., Nagao, J., Minagawa, H., 2015. Lithological features of hydrate-

bearing sediments and their relationship with gas hydrate saturation in the eastern Nankai Trough, Japan. Marine and Petroleum Geology, 66(2), 368-378. DOI: 10.1016/j.marpetgeo.2015.02.022

Kaul, N., Rosenberger, A., Villinger, H., 2000. Comparison of measured and BSR-derived heat flow values, Makranaccretionary prism, Pakistan. Marine Geology, 164(1-2), 37-51. DOI: 10.1016/S0025-3227(99)00125-5

Khain, V.E., Polyakova, I.D., 2004. Oil and gas potential of deep- and ultradeep-water zones of continental margins. Lithology and Mineral Resources, 39(6), 530-540. DOI: 10.1023/B:LIMI.0000046956.08736.e4

Klauda, J.B., Sandler, S.I., 2005. Global distribution of methane hydrate in ocean sediment. Energy & Fuels, 19(2), 459-470. DOI: 10.1021/ef049798o

Kvenvolden, K.A., 1993. Gas hydrates—geological perspective and global change. Reviews of Geophysics, 31(2), 173-187. DOI: 10.1029/93RG00268

Kvenvolden, K.A., 1998. A primer on the geological occurrence of gas hydrates. In: Henriet, J.P., Mienert, J. (eds.). Gas hydrates: Relevance to world margin stability and climate change. The Geological Society of London, Blackwell Scientific, 137 (Special Publications), 9-30. DOI: 10.1144/GSL.SP.1998.137.01.02

Lee, M.W., Collett, T.S., 2012. Pore-and fracture-filling gas hydrate reservoirs in the Gulf of Mexico Gas Hydrate Joint Industry Project Leg II Green Canyon 955 H well. Marine and Petroleum Geology, 34(1), 62-71. DOI: 10.1016/j.marpetgeo.2011.08.002

Li, X.H., Wei, G.J., Shao, L., Liu, Y., Liang, X.R., Jian, Z.M., Sun, M., Wang, P.X., 2003. Geochemical and Nd isotopic variations in sediments of the South China Sea: a response to Cenozoic tectonism in SE Asia. Earth and Planetary Science Letters, 211(3-4), 207-220. DOI: 10.1016/S0012-821X(03)00229-2

Li, Y.M., Luo, X.H., Xu, X., Yang, X.Q., Shi, X.B., 2010. Seafloor in-situ heat flow measurements in the deep-water area of the northern slope, South China Sea (in Chinese with English abstract). Chinese Journal of Geophysics, 53(9), 2161-2170. DOI: 10.3969/j.issn.0001-5733.2010.09.016

Li, H., Wang, Y.M., Zhu, W.L., Xu, Q., He, Y.B., Tang, W., Zhuo, H.T., Wang, D., Wu, J.P., Li, D., 2013. Seismic characteristics and processes of the Plio-Quaternary unidirectionally migrating channels and contourites in the northern slope of the South China Sea. Marine and Petroleum Geology, 43, 370-380. DOI: 10.1016/j.marpetgeo.2012.12.010

Lin, C.C., Lin, A.T.S., Liu, C.S., Homg, C.S., Chen, G.Y., Wang, Y.S., 2014. Canyon-infilling and gas hydrate occurrences in the frontal fold of the offshore accretionary wedge off southern Taiwan. Marine Geophysical Research, 35(1), 21-35. DOI: 10.1007/s11001-013-9203-7

Liu, C.L., Ye, Y.G., Meng, Q.G., He, X.L., Lu, H.L., Zhang, J., Liu, J., Yang, S.X., 2012. The characteristics of gas hydrates recovered from Shenhu Area in the South China Sea. Marine Geology, 307-310, 22-27. DOI: 10.1016/j.margeo.2012.03.004

Lv, C.L., Yao, Y.J., Gong, Y.H., Wu, S.G., Li, X.J., 2012. Deepwater canyons reworked by bottom currents: sedimentary evolution and genetic model. Journal of Earth Science, 23(5), 731-743. DOI: 10.1007/s12583-012-0280-3

MacKay, M., Jarrard, R., Westbrook, G., Hyndman, R.D., 1994. Origin of bottom simulating reflectors: geophysical evidence from the Cascadia accretionary prism. Geology, 22(5), 459-462. DOI: 10.1130/0091-7613(1994)022<0459:OOBSRG>2.3.CO;2

Maslin, M., Owen, M., Day, S., Long, D., 2004. Linking continental-slope failures and climate change: testing the clathrate gun hypothesis. Geology, 32(1), 53-56. DOI: 10.1130/G20114.1

McAdoo, B.G., Pratson, L.F., Orange, D.L., 2000. Submarine landslide geomorphology, US continental slope. Marine Geology, 169, 103-136. DOI: 10.1016/S0025-3227(00)00050-5

Milkov, A.V., 2004. Global estimates of hydrate-bound gas in marine sediments: How much is really out there? Earth-Science Reviews, 66(1-2), 183-197. DOI: 10.1016/j.earscirev.2003.11.002

Miller, P., Dasgupta, S., Shelander, D., 2012. Seismic imaging of migration pathways by advanced attribute analysis, Alaminos Canyon 21, Gulf of Mexico. Marine and Petroleum Geology, 34(1), 111-118. DOI: 10.1016/j.marpetgeo.2011.09.005

Mills, P.C., 1983. Genesis and diagnostic value of soft-sediment deformation structures—a review. Sedimentary Geology, 35(2), 83-104. DOI: 10.1016/0037-0738(83)90046-5

Moscardelli, L., Wood, L., 2008. New classification system for mass transport complexes in offshore Trinidad. Basin Research, 20(1), 73-98. DOI: 10.1111/j.1365-2117.2007.00340.x

Mulder, T., Cochonat, P., 1996. Classification of offshore mass movements. Journal of Sedimentary Research, 66, 43-57. DOI: 10.1306/D42682AC-2B26-11D7-8648000102C1865D

Nissen, S.S., Hayes, D.E., Yao, B.C., Zeng, W.J., Chen, Y.Q., Nu, X.P., 1995. Gravity, heat flow, and seismic constraints on the processes of crustal extension: northern margin of the South China Sea. Journal of Geophysical Research: Solid Earth, 100(B11), 22447-22483. DOI: 10.1029/95JB01868

Noguchi, S., Shimoda, N., Takano, O., Oikawa, N., Inamori, T., Saeki, T., Fujii, T., 2011. 3-D internal architecture of methane hydrate-bearing turbidite channels in the eastern Nankai Trough, Japan. Marine and Petroleum Geology, 28, 1817-1828. DOI: 10.1016/j.marpetgeo.2011.02.004

Normark, W.R., Gutmacher, C.E., Chase, T.E., Wilde, P., 1985. Monterey Fan, Pacific Ocean. In: Bouma, A.H., Normark, W.R., Barnes, N.E. (eds.). Submarine fans and related turbidite systems. New York Springer-Verlag, 79-86pp. DOI: 10.1007/978-1-4612-5114-9_13

Passega, R., 1964. Grain size representation by Cm Patterns as a geological tool. Journal of Sedimentary Petrology, 34(4), 830-847. DOI: 10.1306/74D711A4-2B21-11D7-8648000102C1865D

Qiao, S.H., Su, M., Yang, R., Su, P.B., Kuang, Z.G., Liang, J.Q., Wu, N.Y., 2014. A comparative study on the difference of fluil migration between the Shenhu and LW3-1 drilling areas for natural gas hydrate, northern South China Sea (in Chinese with English abstract). Natural Gas Industry, 34(10), 137-143. DOI: 10.3787/j.issn.1000-0976.2014.10.022

Qiao, S.H., Su, M., Kuang, Z.G., Yang, R., Liang, J.Q., Wu, N.Y., 2015. Canyon-related undulation structures in the Shenhu area, northern South China Sea. Marine Geophysical Researches, 36(2), 243-252. DOI: 10.1007/s11001-015-9252-1

Rajan, A., Bünz, S., Mienert, J., Smith, A.J., 2013. Gas hydrate systems in petroleum provinces of the SW-Barents Sea. Marine and Petroleum Geology, 46, 92-106. DOI: 10.1016/j.marpetgeo.2013.06.009

Riedel, M., Hyndman, R.D., Spence, G.D., Chapman, N.R., 2002. Seismic investigations of a vent field associated with gas hydrates, offshore Vancouver Island. Journal of Geophysical Research: Solid Earth, 107(B9), 5-1 5-16. DOI: 10.1029/2001JB000269

Riedel, M., Collett, T.S., Shankar, U., 2011. Documenting channel features associated with gas hydrates in the Krishna–Godavari Basin, Offshore India. Marine Geology, 279(1), 1-11. DOI: 10.1016/j.margeo.2010.10.008

Riedel, M., Bahk, J.J., Scholz, N.A., Ryu, B.J., Yoo, D.G., Kim, W., Kim, G.Y., 2012. Mass-transport deposits and gas hydrate occurrences in the Ulleung Basin, East Sea–Part 2: Gas hydrate content and fracture-induced anisotropy. Marine and Petroleum Geology, 35(1), 75-90. DOI: 10.1016/j.marpetgeo.2012.03.005

Riedel, M., Bahk, J.J., Kim, H.S., Scholz, N.A., Yoo, D.G., Kim, W.S., Ryu, B.J., Lee, S.R., 2013a. Seismic facies analyses as aid in regional gas hydrate assessments. Part-II: Prediction of reservoir properties, gas hydrate petroleum system analysis, and Monte Carlo simulation. Marine and Petroleum Geology, 47, 269-290. DOI: 10.1016/j.marpetgeo.2013.04.012

Riedel, M., Collett, T.S., Kim, H.S., Bahk, J.J., Kim, J.H., Ryu, B.J., Kim, G.Y., 2013b. Large-scale depositional characteristics of the Ulleung Basin and its impact on electrical resistivity and Archie-parameters for gas hydrate saturation estimates. Marine and Petroleum Geology, 47, 222-235. DOI: 10.1016/j.marpetgeo.2013.03.014

Ru, K., Pigott, J.D., 1986. Episodic rifting and subsidence in the South China Sea. American Association of Petroleum. Geologists Bulletin, 70(9), 1136-1155.

Sain, K., Gupta, H., 2012. Gas hydrates in India: Potential and development. Gondwana Research, 22(2), 645-657. DOI: 10.1016/j.gr.2012.01.007

Scholz, N.A., Riedel, M., Bahk, J.J., Yoo, D.G., Ryu, B.J., 2012. Mass transport deposits and gas hydrate occurrences in the Ulleung Basin, East Sea–Part 1: Mapping sedimentation patterns using seismic coherency. Marine and Petroleum Geology, 35(1), 91-104. DOI: 10.1016/j.marpetgeo.2012.03.004

Shankar, U., Riedel, M., 2010. Seismic and heat flow constraints from the gas hydrate system in the Krishna–Godavari Basin, India. Marine Geology, 276(1), 1-13. DOI: 10.1016/j.margeo.2010.06.006

Shanmugam, G., 2006. Deep-water processes and facies models: implications for sandstone petroleum reservoirs. Handbook of petroleum exploration and production. Amsterdam, Elsevier, 476pp. ISBN: 0444521615

Shedd, W., Boswell, R., Frye, M., Godfriaux, P., Kramer, K., 2012. Occurrence and nature of "bottom simulating reflectors" in the northern Gulf of Mexico. Marine and Petroleum Geology, 34(1), 31-40. DOI: 10.1016/j.marpetgeo.2011.08.005

Shi, X.B., Qiu, X.L., Xia, K.Y., Zhou, D., 2003. Characteristics of surface heat flow in the South China Sea. Journal of Asian Earth Sciences, 22(3), 265-277. DOI: 10.1016/S1367-9120(03)00059-2

Shipley, T.H., Houston, M.H., Buffler, R.T., Shaub, F.J., McMillen, K.J., Ladd, J.W., Worzel, J.L., 1979. Seismic evidence for widespread possible gas hydrate horizons on continental slopes and rises. American Association of Petroleum Geologists Bulletin, 63, 2204-2213.

Sloan, E.D., Koh, C.A., 2008. Clathrate hydrates of natural gases (third edition). New York, CRC Press, Taylor and Francis Group, Publishers, 721pp. ISBN: 0849390788 9780849390784 9781420008494

Stow, D.A.V., Mayall, M., 2000. Deep-water sedimentary systems: new models for the 21st century. Marine and Petroleum Geology, 17(2), 125-135. DOI:10.1016/S0264-8172(99)00064-1

Su, M., Yang, R., Zhang, C.M., Cong, X.R., Liang, J.Q., Sha, Z.B., 2013. Progress in study of deep-water depositional system in the northern continental slope of the South China Sea and its implications for gas hydrate research (in Chinese with English abstract). Marine Geology & Quaternary Geology, 33, 109-116.

Su, M., Yang, R., Wu, N.Y., Wang, H.B., Liang, J.Q., Sha, Z.B., Cong, X.R., Qiao, S.H., 2014a. Structural characteristics in the Shenhu Area, northern continental slope of South China Sea, and their influences on gas hydrate (in Chinese with English abstract). Acta Geologica Sinica, 88(3), 318-326.

Su, M., Yang, R., Wu, N.Y., Zhang, H., Qiao, S.H., Cong, X.R., Sha, Z.B., Liang, J.Q., Kuang, Z.G., Su, P.B., 2014b. Erosional-sedimentary controls on the accumulation and distribution of gas hydrate in the Shenhu Area, northern slope of the South China Sea. Beijing (China), 8th International Conference on Gas Hydrates (ICGH 2014), 28 Jul-1 Aug 2014, 1-14.

Su, P.B., Liang, J.Q., Sha, Z.B., Fu, S.Y., Lei, H.Y., Gong, Y.H., 2011. Dynamic simulation of gas hydrate reservoirs in the Shenhu area, the northern South China Sea (in Chinese with English abstract). Acta Petrolei Sinica, 32(2), 226-233. DOI: 10.7623/syxb201102006

Su, Z., Cao, Y.C., Yang, R., Wu, N.Y., Yang, S.X., Wang, H.B., 2012. Analytical research on evolution of methane hydrate deposits at Shenhu Area, northern South China Sea (in Chinese with English abstract). Chinese Journal of Geophysics, 55, 1764-1774.

Sultan, N., Cochonat, P., Foucher, J.P., Mienert, J., 2004. Effect of gas hydrates melting on seafloor slope instability. Marine Geology, 213(1-4), 379-401. DOI: 10.1016/j.margeo.2004.10.015

Sun, Q.L., Wu, S.G., Cartwright, J., Dong, D.D., 2012a. Shallow gas and focused fluid flow systems in the Pearl River Mouth Basin, northern South China Sea. Marine Geology, 315-318, 1-14. DOI: 10.1016/j.margeo.2012.05.003

Sun, Y.B., Wu, S.G., Dong, D.D., Lüdmann, T., Gong, Y.H., 2012b. Gas hydrates associated with gas chimneys in fine-grained sediments of the northern South China Sea. Marine Geology, 311-314, 32-40. DOI: 10.1016/j.margeo.2012.04.003

Torres, M.E., Tréhu, A.M., Cespedes, N., Kastner, M., Wortmann, U.G., Kim, J.H., Long, P., Malinverno, A., Pohlman, J.W., Riedel, M., Collett, T.S., 2008. Methane hydrate formation in turbidite sediments of northern Cascadia, IODP Expedition 311. Earth and Planetary Science Letters, 271(1-4), 170-180. DOI: 10.1016/j.epsl.2008.03.061

Tréhu, A.M., Ruppel, C., Holland, M., Dickens, G.R., Torres, M.E., Collett, T.S., Goldberg, D., Riedel, M., Schultheiss, P., 2006. Gas hydrates in marine sediments: lessons from scientific ocean drilling. Oceanography, 19(4), 124-142. DOI: 10.5670/oceanog.2006.11

Tsuji, Y., Ishida, H., Nakamizu, M., Matsumoto, R., Shimizu, S., 2004. Overview of the MITI Nankai Trough wells: A milestone in the evaluation of methane hydrate resources. Resource Geology, 54(1), 3-10. DOI: 10.1111/j.1751-3928.2004.tb00182.x

Van Loon, A.J., Brodzikowski, K., 1987. Problems and progress in the research on soft-sediment deformations. Sedimentary Geology, 50(1-3), 167-193. DOI: 10.1016/0037-0738(87)90032-7

Walker, R.G., 1978. Deep-water sandstone facies and ancient submarine fans: models for exploration for stratigraphic traps. American Association of Petroleum Geologists Bulletin, 62, 932-966.

Wallmann, K., Pinero, E., Burwicz, E., Haeckel, M., Hensen, C., Dale, A., Ruepke, L., 2012. The global inventory of methane hydrate in marine sediments: A theoretical approach. Energies, 5(7), 2449-2498. DOI: 10.3390/en5072449

Wang, D.W., Wu, S.G., Qin, Z.L., Ding, W.W., Cao, Q.B., 2009. Architecture and identification of large Quaternary mass transport depositions in the slope of South China Sea (in Chinese with English abstract). Marine Geology & Quaternary Geology, 29, 65-72.

Wang, L.F., Sha, Z.B., Liang, J.Q., Lu, J.A., 2010. Analysis of gas hydrate absence induced by the late-stage diaper domination in the borehole SH5 of Shenhu Area (in Chinese with English abstract). Geoscience, 24(3), 450-456. DOI: 10.3969/j.issn.1000-8527.2010.03.005

Wang, H.R., Wang, Y.M., Qiu, Y., Peng, X.C., Li, W.C., 2007. The sediment waves in the deep-water setting in the northern continental slope of the South China Sea (in Chinese with English abstract). Progress in Natural Science, 17(9), 1235-1243. DOI: 10.3321/j.issn:1002-008x.2007.09.012

Wang, P., Zhang, X., Zhu, Y., Li, B., Huang, X., Pang, S., Zhang, S., Lu, C., Xiao, R., 2014. Effect of permafrost properties on gas hydrate petroleum system in the Qilian Mountains, Qinghai, Northwest China. Environmental Sciences. Processes & Impacts, 16, 2711-20. DOI: 10.1039/c4em00482e

Wang, X.J., Wu, S.G., Yuan, S.Q., Wang, D.W., Ma, Y.B., Yao, G.S., Gong, Y.H., Zhang, G.X., 2010. Geophysical signatures associated with fluid flow and gas hydrate occurrence in a tectonically quiescent sequence, Qiongdongnan Basin, South China Sea. Geofluids, 10(3), 351-368. DOI: 10.1111/j.1468-8123.2010.00292.x

Wang, X.J., Lee, M., Collett, T.S., Yang, S.X., Guo, Y.Q., Wu, S.G., 2014a. Gas hydrate identified in sand-rich inferred sedimentary section using downhole logging and seismic data in Shenhu area, South China Sea. Marine and Petroleum Geology, 51, 298-306. DOI: 10.1016/j.marpetgeo.2014.01.002

Wang, X.J., Collett, T.S., Lee, M.W., Yang, S.X., Guo, Y.Q., Wu, S.G., 2014b. Geological controls on the occurrence of gas hydrate from core, downhole log, and seismic data in the Shenhu area, South China Sea. Marine Geology, 357, 272-292. DOI: 10.1016/j.margeo.2014.09.040

Weimer, P., Roger, M.S., 2004. Petroleum systems of deepwater settings. Tulsa, Society of Exploration Geophysicists and European Association of Geoscientists & Engineers Publishers, 470pp. DOI: 10.1190/1.9781560801955

Wood, W.T., Ruppel, C., 2000. Seismic and thermal investigations of the Blake Ridge gas hydrate area: a synthesis. Proceedings of the Ocean Drilling Program. Scientific results, 164, 253-264.

Wu, N.Y., Yang, S.X., Zhang, H.Q., Liang, J.Q., Wang, H.B., Su, X., Fu, S.Y., 2008. Preliminary discussion on natural gas hydrate reservoir system of Shenhu area, north Slope of South China Sea. Vancouver B.C. (Canada), 6th International Conference on Gas Hydrates (ICGH 2008), 6-10 July 2008, 1-7.

Wu, N.Y., Yang, S.X., Wang, H.B., Liang, J.Q., Gong, Y.H., Lu, Z.Q., Wu, D.D., Guan, H.X., 2009. Gas bearing fluid influx sub-system for gas hydrate geological system in Shenhu Area, northern South China Sea (in Chinese with English abstract). Chinese Journal of Geophysics, 52(6), 1641-1650. DOI: 10.3969/j.issn.0001-5733.2009.06.027

Wu, N.Y., Zhang, H.Q., Yang, S.X., Zhang, G.X., Liang, J.Q., Lu, J.A., Su, X., Schultheiss, P., Holland, M., 2011. Gas hydrate system of Shenhu Area, northern South China Sea: geochemical results. Journal of Geological Research, 2011, 1-10. DOI: 10.1155/2011/370298

Wu, S.G., Zhang, G.X., Huang, Y.Y., Liang, J.Q., Wong, H.K., 2005. Gas hydrate occurrence on the continental slope of the northern South China Sea. Marine and Petroleum Geology, 22(3), 403-412. DOI: 10.1016/j.marpetgeo.2004.11.006

Wu, S.G., Wang, X.J., Wong, H.K., Zhang, G.X., 2007. Low-amplitude BSRs and gas hydrate concentration on the northern margin of the South China Sea. Marine Geophysical

Researches, 28(2), 127-138. DOI: 10.1007/s11001-007-9020-y

Wynn, R.B., Stow, D.A.V., 2002. Classification and characterisation of deep-water sediment waves. Marine Geology, 192(1-3), 7-22. DOI: 10.1016/S0025-3227(02)00547-9

Xu, X., Li, Y.M., Luo, X.H., Shi, X.B., Yang, X.Q., 2012. Comparison of different-type heat flows at typical sites in natural gas hydrate exploration area on the northern slope of the South China Sea (in Chinese with English abstract). Chinese Journal of Geophysics, 55(3), 998-1006. DOI: 10.6038/j.issn.0001-5733.2012.03.030

Yang, R., Su, M., Qiao, S.H., Cong, X.R., Su, Z., Liang, J.Q., Wu, N.Y., 2015. Migration of methane associated with gas hydrates of the Shenhu Area, northern slope of South China Sea. Marine Geophysical Researches, 36(2), 253-261. DOI: 10.1007/s11001-015-9249-9

Yang, S.X., Zhang, H.Q., Wu, N.Y., Su, X., Schultheiss, P., Holland, M., Zhang, G.X., Liang, J.Q., Lu, J.A., Rose, K., 2008. High concentration hydrate in disseminated forms obtained in Shenhu area, North Slope of South China Sea. Vancouver B.C. (Canada), 6th International Conference on Gas Hydrates (ICGH 2008), 6-10 July 2008, 1-6.

Yu, X.H., Liang, J.Q., Fang, J.N., Cong, X.R., Jiang, L.Y., Wang, J.Z., 2012. Tectonic subsidence characteristics and its relationship to BSR distribution in deep water area of Pearl River Mouth Basin since the Late Miocene (in Chinese with English abstract). Journal of Palaeogeography, 6, 787-800. DOI: 10.7605/gdlxb.2012.06.010

Yu, X.H., Wang, J.Z., Liang, J.Q., Li, S.L., Zeng, X.M., Li, W., 2014. Depositional characteristics and accumulation model of gas hydrates in northern South China Sea. Marine and Petroleum Geology, 56, 74-86. DOI: 10.1016/j.marpetgeo.2014.03.011

Yuan, Y.S., Zhu, W.L., Mi, L.J., Zhang, G.C., Hu, S.B., He, L.J., 2009. "Uniform geothermal gradient" and heat flow in the Qiongdongnan and Pearl River Mouth Basins of the South China Sea. Marine and Petroleum Geology, 26(7), 1152-1162. DOI: 10.1016/j.marpetgeo.2008.08.008

Zhang, G.X., Huang, Y.Y., Zhu, Y.H., Wu, B.H., 2002. Prospect of gas hydrate resources in the South China Sea (in Chinese with English abstract). Marine Geology & Quaternary Geology, 22, 75-81.

Zhang, G.X., Chen, F., Yang, S.X., Su, X., Sha, Z.B., Wang, H.B., Liang, J.Q., Zhou, Y., 2012. Accumulation and exploration of gas hydrate in deep-sea sediments of northern South China Sea. Chinese Journal of Oceanology and Limnology, 30(5), 876-888. DOI: 10.1007/s00343-012-1313-6

Zhang, P.Z., Molnar, P., Downs, W.R., 2001. Increased sedimentation rates and grain sizes 2–4Myr ago due to the influence of climate change on erosion rates. Nature, 410, 891-897. DOI: 10.1038/35073504

Zhang, S.L., Chen, D.F., Huang, J.Q., 2007. Conditions of accumulation of gas hydrate in Baiyun Sag (in Chinese with English abstract). Natural Gas Industry, 27, 7-10.

Zhu, M.Z., Graham, S., Pang, X., McHargue, T., 2010. Characteristics of migrating submarine canyons from the middle Miocene to present: implications for paleoceanographic circulation, northern South China Sea. Marine and Petroleum Geology, 27(1), 307-319. DOI: 10.1016/j.marpetgeo.2009.05.005

Zhu, W.L., Huang, B.J., Mi, L.J., Wilkins, R.W.T., Fu, N., Xiao, X.M., 2009. Geochemistry, origin, and deep-water exploration potential of natural gases in the Pearl River Mouth and Qiongdongnan basins, South China Sea. American Association of Petroleum Geologists Bulletin, 93(6), 741-761. DOI: 10.1306/02170908099

Zhu, Y.H., Huang, X., Fu, S.Y., Su, P.B., 2013. Gas sources of natural gas hydrates in the Shenhu Drilling Area, South China Sea: geochemical evidence and geological analysis. Acta Geologica Sinica, 87(3), 767-776. DOI: 10.1111/1755-6724.12088

Manuscript received December 2014;
revision accepted October 2015;
published Online March 2016.